



**MODELS FOR INVESTIGATION OF
ELECTROLUMINESCENCE FROM SILICON
AND GERMANIUM NANOSTRUCTURES**

By
Getnet Melese

SUBMITTED IN PARTIAL FULFILLMENT OF THE
REQUIREMENTS FOR THE DEGREE OF
MASTER OF SCIENCE IN PHYSICS

AT

ADDIS ABABA UNIVERSITY
ADDIS ABABA, ETHIOPIA

JUNE, 2009

ADDIS ABABA UNIVERSITY
DEPARTMENT OF
PHYSICS

The undersigned hereby certify that they have read and recommend to the Faculty of Graduate Studies for acceptance a thesis entitled “ **Models for investigation of Electroluminescence from Silicon and Germanium nanostructures**” by **Getnet Melese** in partial fulfillment of the requirements for the degree of **Master of Science in physics**.

Dated: June, 2009

Advisor:

Dr. S. K. Ghoshal

Examiners:

Prof. P. Singh

Dr. Tesgera Bedassa

ADDIS ABABA UNIVERSITY

Date: **June, 2009**

Author: **Getnet Melese**

Title: **Models for investigation of Electroluminescence from
Silicon and Germanium nanostructures**

Department: **Physics**

Degree: **M.Sc.** Convocation: **June** Year: **2009**

Permission is herewith granted to Addis Ababa University to circulate and to have copied for non-commercial purposes, at its discretion, the above title upon the request of individuals or institutions.

Signature of Author

THE AUTHOR RESERVES OTHER PUBLICATION RIGHTS, AND NEITHER THE THESIS NOR EXTENSIVE EXTRACTS FROM IT MAY BE PRINTED OR OTHERWISE REPRODUCED WITHOUT THE AUTHOR'S WRITTEN PERMISSION.

THE AUTHOR ATTESTS THAT PERMISSION HAS BEEN OBTAINED FOR THE USE OF ANY COPYRIGHTED MATERIAL APPEARING IN THIS THESIS (OTHER THAN BRIEF EXCERPTS REQUIRING ONLY PROPER ACKNOWLEDGEMENT IN SCHOLARLY WRITING) AND THAT ALL SUCH USE IS CLEARLY ACKNOWLEDGED.

To my father whom I lost on November 28, 2009, with the help of god I able to withstand my condolences and complete this thesis and my graduate study.

Table of Contents

Table of Contents	vi
List of Figures	vii
Abstract	ix
Acknowledgements	x
1 Introduction	1
1.1 Thesis outline and objectives	4
2 Quantum confinement and band structures	5
2.1 Introduction	5
2.1.1 Quantum dots	5
2.1.2 Quantum wires (nanowires)	6
2.1.3 Quantum wells (QW)	8
2.1.4 Density of state in low dimensional structures	8
2.2 Band structures of Si and Ge nanostructures	9
2.2.1 Tight binding approximations	10
2.2.2 The pseudo potential method (PPM)	13
2.3 Excitons	16
3 Optical and electrical properties of Si and Ge nanostructures	18
3.1 Porous silicon preparation	18
3.1.1 Emission and absorption of light	18
3.2 Luminescence	20
3.2.1 Recombination rates	21
3.3 Photoluminescence	22
3.3.1 The photoluminescence of porous silicon	22
3.4 Electroluminescence	24
3.4.1 Practical applications	24
3.4.2 Types of electroluminescence	25
3.4.3 Fundamental physical processes	26

3.4.4	Injection electroluminescence	26
4	Luminescence through impurities in Si and Ge nanostructures	28
4.1	Introduction	28
4.2	Silicon nanocrystals in SiO ₂	29
4.3	EL signal enhancement by hydrogen passivation	33
4.4	Electroluminescence and photoluminescence of Ge-implanted Si/SiO ₂ and Si structures	35
4.5	Transmission measurement of EL	36
4.6	Dependence of EL intensity on temperature	37
4.6.1	Temperature Dependence of EL for Si impurities	38
4.7	Transient properties of EL and its degradation	39
4.7.1	Electroluminescence degradation	39
5	Formulation of models	41
5.1	The quantum confinement model (QCM)	41
5.2	Surface state model (SSM)	44
5.2.1	Interface states model (ISM)	45
6	Results and discussion	47
6.1	Dependence of PL intensity on wavelength for different σ s	47
6.2	Dependence of EL intensity on wavelength for different σ s	48
6.3	EL intensity and number of sample atoms for Si and Ge nanostructures	50
6.4	EL intensity and voltage	51
6.5	EL intensity and wavelength for oxygen terminated Si nanocluster	51
6.6	EL intensity and wavelength for H-terminated Si nanocluster	52
6.7	Dependence of EL intensity on Si-O bonds	53
6.8	Dependence of EL intensity on applied voltage for O-terminated Si	54
6.9	EL intensity versus Si-H bonds and voltage	55
6.10	Dependence of EL intensity on temperature and current density	55
7	Conclusion and future outlook	58
	Bibliography	60

List of Figures

2.1	Change in density of state as the number of confining dimension increases .	9
2.2	The actual potential and the pseudo potential with their corresponding wave functions [7]	15
2.3	Exciton levels for transition from VB to CB [7]	16
3.1	Direct and indirect band transitions [15]	19
3.2	Electron -hole structures in semiconductors [25]	24
4.1	Visible light spectrum [39]	29
4.2	Different wavelength of electromagnetic spectrum [39]	30
4.3	Bond structures of Si and O [26, 41,42]	31
4.4	Device set up for electroluminescence measurements [40]	35
4.5	EL and PL intensities measured at 950 nm as a function of temperature. The EL intensity is measured with current density of 0.16 A/cm ² and the PL intensity with a 488 nm pump laser power of 10 mW [34]	37
6.1	PL intensity versus wavelength for Si and Ge nanostructures	48
6.2	EL intensity as a function of wavelength for Si and Ge nanostructures	49
6.3	EL intensity versus wavelength taken for comparison [38]	49
6.4	EL intensity versus number of Si and Ge nanoclusters	50
6.5	EL intensity versus applied voltage for Si and Ge nanoclusters	51
6.6	EL intensity as a function of wavelength for O-passivated Si nanoclusters .	52
6.7	EL intensity as a function of wavelength for H-passivated Si nanoclusters .	53
6.8	EL intensity versus number sample Si-O bonds	53
6.9	EL intensity as a function of applied voltage for O-passivated Si nanocluster	54
6.10	EL intensity vs wavelength for H-passivation	55

6.11 EL and PL intensities vs temperature	56
6.12 Current density vs temperature	56

Abstract

Bulk silicon (Si) and germanium (Ge) have an indirect band gap transitions; however when they are miniaturized to nanometric scale, the energy gap between the highest occupied molecular orbital (HOMO) and the lowest unoccupied molecular orbital (LUMO) increases, and hence the transition changes to direct due to confinement. The HOMO-LUMO gap determines the excitation of electrons so that the nanostructures will emit light.

In this thesis, quantum confinement effects for Si and Ge, some methods of calculating band structures, comparative analysis of photoluminescence (PL) and electroluminescence (EL) are presented. The thesis focuses on EL and for comparison purpose, some studies on PL is touched. Both are the emission of energy in the form of light spectrum of different wavelength by optical radiation, and current or strong electric field.

The dependence of EL on different parameters like size of the nanocluster, applied voltage, band gap energy, wavelength, temperature, and time for Si are briefly examined. The dielectric matrix silicon dioxide has unique optical and electrical properties, as a result the dependence of EL intensity on the above parameters for Si-terminated with oxygen and hydrogen is included in the thesis; in fact passivation enhances EL and highly efficient EL is obtained at low operating voltages ($< 6V$), it is also observed that EL degrades with time. The EL and PL intensities occur at the same energy, however the EL intensity has sharp Gaussian peak and red shifted compared to the PL intensity. To get our result, we used the idea of quantum confinement model (QCM) and surface state model (SSM), that can explain PL and EL on pure Si nanostructures, and Si-terminated with impurities. Our results are consistent with experimental reports.

Acknowledgements

I am grateful to my advisor, Dr. S. K. Ghoshal for his critical and constructive suggestion, well planned follow up, constant support, and friendly approach during this research, he was tireless, programmed, and ready to encourage me at any time when I consult him not only in my thesis work but also in my entire graduate study. As an advisor he put a lot of impression on me that I never forget whenever and wherever in my academic life; I want to forward my gratitude to Mr. Anteneh Getachew and Mr. Billilign Tsigie for their unreserved academical and technical support; with out the help of these persons the work could not be completed duly.

I am indebted to express my heart felt gratitude to the following individuals, who have been electronic communications with me for providing journals and other materials related to my thesis; Mr. Ayesheshim Kebie from Alberta University, Canada, Dr. Asdesach Zenamarkos from Germany, Mr. Getasew Admasu from Antwerp University, Belgium and Mr. Semere Ayalew from Jimma University.

I want to express my due appreciation to Addis Ababa University, physics department, for providing this chance, rendering good office service during my stay, and I want to extend my acknowledgement to the staff members of the department, who devote their time for academic matters that made my stay very happy in the graduate program.

Finally, with no words for me to express my heart feeling for his patience, I would deeply like to thank Mr. Solomon H/M, for his great cooperation on conducting many of my affairs directly or indirectly related to Jimma University on behalf of me and I want to extend my gratitude to Jimma University, providing sponsorship, for faculty of education, and Physics department for creating conducive situations to get sponsorship from the University to my study.

**Models for investigation of
Electroluminescence from Silicon and
Germanium nanostructures**

Getnet Melese

June 30, 2009

Chapter 1

Introduction

Nanotechnology has yielded a number of unique structures that are not found anywhere in nature. Quantum confinement, demonstrates the essential features of small size, the sizes should be < 30 nm for effective confinement. Confinement is so important, because it leads to new electronic properties that are not present in today's semiconductor devices. For instance, the typical quantum dot (QD) which exhibits 0-D confinement is anywhere between 3-60 nm in diameter, it can be loosely described as an 'artificial atom'. QDs are too small and too difficult to isolate in an experiment, but still large enough to be manipulated by magnetic fields and can even be moved around with scanning tunneling microscopy (STM) or atomic force microscopy (AFM).

Confinement can also increase the efficiency of today's electronics. The laser based on a 2-D confinement layer that is usually created with some form of epitaxy like molecular beam epitaxy (MBE) or chemical vapor decomposition (CVD). The bulk of modern lasers created with this method are highly functional, but ultimately inefficient in terms of energy consumption and heat dissipation.

There are several structures like nanotubes and bucky balls that are academically interesting. A carbon nanotube for instance, has drawn much attention as one of the principal nanostructures that exhibit some great potential in nano-electro-mechanical systems (NEMS) [1].

Silicon (Si) is the material of choice in microelectronic industry. This remarkable success is due to various factors such as the wide availability of Si and the ease of producing the natural silicon oxide (SiO_2). Si has good thermal and mechanical properties that make it easy to handle, manufacture, and facilitate the processing of Si based devices. On the other hand SiO_2 is an excellent insulator and can effectively passivate the Si surface. Also there is a very high etching selectivity of SiO_2 with respect to Si. The remarkable properties of Si and SiO_2 make possible the integration of an increasing number of devices on ever larger Si wafers [2].

In their last report, the international road map for semiconductors (ITRS), states that total interconnection length for one processor is presently 1.5 km/cm^2 but will exceed 5 km/cm^2 in about ten years, incurring significant propagation delays, overheating and information latency. According to the ITRS, present manufacturing technology can not address this problem after 2010. It has been realized that the integration of optoelectronic components on all Si matrix would considerably simplify the conception and fabrication of integrated optoelectronic devices [3]. However Si is a poor light emitter because of its indirect band gap impedes radiative transitions. Its use in optoelectronics is very limited, especially for light emitting devices such as light emitting diodes (LEDs) and solid state (Si) lasers, the latter being a starting point of many optoelectronic devices [4].

Si and Ge are the most common metalloids, the conduction and valence bands of Ge are based on a combination of theoretical and experimental results [5]. Si is a tetravalent metalloid and less reactive than its chemical analog carbon, occurs as a pure element in nature, and the eighth most common element in the universe by mass, more widely distributed in dusts, planetoids and planets as various forms of SiO_2 . It is widely used in semiconductors because, it remains semiconductor at higher temperatures than the semiconductor Ge and because of its native oxide it is easily grown in furnace and forms a better semiconductor/dielectric interface than any other material [6].

The threshold of optical absorption at frequency ω_g determines the band gap $E_g = \hbar\omega_g$.

In the direct absorption process, a photon is absorbed by the crystal with the creation of an electron and a hole. In indirect absorption process, the minimum energy gap of the band structure involves electrons and holes separated by substantial wave vector k . Here in a direct photon transition at energy of the minimum gap can not satisfy the requirement of conservation of wave vector, because photon wave vectors are negligible at the energy range of interest.

Optical measurements determine whether the band gap is direct or indirect. The band gap in bulk Ge and Si are connected by indirect transitions, light emission in these materials are naturally phonon mediated process (spontaneous recombination life times in the millisecond range) [7]. Silicon nanowire (SiNW) growth with hydrogen passivation has been demonstrated and extensive experimental and theoretical studies of electronic, optical, and mechanical properties have been performed. SiNWs have a direct band gap, with potential applications in electronic, optoelectronic, and chemical sensors [8].

Si is the leading material concerning high density electronic functionality, its band gap (1.12 eV) is ideal for room temperature operation, and its oxide (SiO_2 allows a processing flexibility to place more than 10^8 transistors on a single chip). However all the single transistors and electronic devices have to transfer information on length scales which are relevant with respect to their nanometric scale. In bulk Si competitive non-radiative recombination rates are much higher than the radiative ones and most of the excited electron-hole (e-h) pairs recombine non-radiatively. This yields a very low internal quantum efficiency for Si luminescence. As what concerns the lasing of Si, fast non-radiative process such as Auger or free carrier absorption severely prevent population inversion at high pumping rates needed to achieve optical amplification [9]. The alloy composition of Si and Ge remains indirect, there is a little motivation from optoelectronic device considerations to grow the alloy; however, there has been great interest in this alloy since it can be a component of Si-SiGe structures and allow hetrostructure concepts to be realized in Si technology [10].

1.1 Thesis outline and objectives

In this thesis we study the optical and electrical properties of Si and Ge nanostructures with more emphasis on electrical properties. The thesis is organized in six chapters apart from the introduction; chapter 2 deals with quantum confinement and band structures, in this chapter quantum wells, quantum wires and quantum dots as well as some of the methods of calculating band structures like the tight binding and the pseudo potential are discussed. Chapter 3 contains optical and electrical properties of Si and Ge nanostructures; here emission and absorption of light, recombination rates, EL and PL of porous silicon are presented. Chapter 4 is concerned mainly about luminescence from Si terminated with O and H. Here more attention is given when Si is embedded in a dielectric SiO_2 . Chapters 5 and 6 talk about the formulation of models and results of this work respectively. The last chapter gives conclusion and future outlooks.

General and specific objectives

The general objective of this work is to study EL intensity using QC model and SSM.

Specific objectives

- To describe the dependence of band gap transitions of Si and Ge on their size
- To study the dependence of EL intensity on different parameters
- To compare and contrast the relation between EL and PL from Si and Ge nanostructures
- To study the effect of applied voltage and current density on the quantum efficiency and EL intensity

Chapter 2

Quantum confinement and band structures

2.1 Introduction

In this chapter we will discuss the dependence of band gap energy on the confined dimensions, and some of the methods of calculating electronic band structures.

2.1.1 Quantum dots

Quantum dots (QDs) are nanometer scale "boxes" for selectively holding or releasing electrons. They are small physical devices that contain a "tiny droplet" of free electrons, small metal or semiconductor boxes that hold a specified number of electrons (QDs generally look more like pyramids than actual dots). QDs are grouping of atoms so small that the addition or removal of an electron will change its properties in a significant way. QDs are semiconductor structures where the electron wave function is confined in all three dimensions by the potential energy barriers that form the QDs boundaries. Specifically, QDs are semiconductor structures that confine the electrons and holes to a volume of order of 20 nm^3 .

Modern semiconductor processing techniques permit the artificial creation of quantum confinement (quantum confinement in all three spatial dimensions) of only few electrons;

such a finite fermions QD systems have much in common with the atoms, yet they are man made structures, designed and fabricated in the laboratory.

The generalization of the Schrodinger equation in three dimension is:

$$-\frac{\hbar^2}{2m}\nabla^2\Psi(r) + V(r)\Psi(r) = E\Psi(r) \quad (2.1.1)$$

The solution of the differential eq.(2.1.1) for a particle in 3D infinite trap of volume L^3 with impermeable walls with $V(r) = 0$ is given as:

$$\Psi_n(x, y, z) = \left(\frac{2}{L}\right)^{\frac{3}{2}} \sin\left(\frac{n_x\pi x}{L}\right) \sin\left(\frac{n_y\pi y}{L}\right) \sin\left(\frac{n_z\pi z}{L}\right) \quad (2.1.2)$$

and the corresponding energy eigen value will be

$$E_n = \frac{\hbar^2\pi^2}{2mL^2}(n_x^2 + n_y^2 + n_z^2) \quad (2.1.3)$$

Eqs.(2.1.2) and (2.1.3) are applicable to electron and hole states in semiconductor” quantum dots”.

A”hole”(missing electron) in a full energy band behaves very much like an electron except that it has a positive charge, and tends to float to the top of the band, i.e the energy of the hole increases oppositely to the energy of an electron. To create an electron hole pair in semiconductors requires energy at least equal to the energy gap E_g of the semiconductor.

2.1.2 Quantum wires (nanowires)

Nanowires (also called quantum wires) are 1D molecular structure with electrical and/or optical properties. In order to have enhanced physical properties, the wires must be of small diameter, must have high aspect ratio (i.e. the ratio of length to thickness), and must be uniformly oriented. Nanowires are relatively easy to produce and can have

different shapes. They are often thin and short "threads" but can also have other manifestations. The propagation of electromagnetic energy has been demonstrated along noble metal stripes with band of a few microns, propagation has also been demonstrated along nanowires with sub wavelength cross sections and propagation length of a few micron. Metal nanowires can also be used to "transmit" photons. The optical properties of metal nanowires can be optimized for particular wavelength of interest, and non-regular cross-sections and coupling between closely spaced nanowires allows a tunneling of optical response.

The term quantum wire describes a carrier confined in two dimensions say Y and Z to a small dimension d (wire cross-section d) and free to move along the length of the wire X (qualitatively this situation resembles the situation of the carrier moving along a carbon nanotube, or silicon nanowire, although the details of the bound state wave functions are different).

The solution of eq.(2.1.1) in the case of quantum wire of a square cross-section is

$$\Psi_{nn}(x, y, z) = \left(\frac{2}{d}\right) \sin\left(\frac{n_y \pi y}{d}\right) \sin\left(\frac{n_z \pi z}{d}\right) \exp(iK_x X) \quad (2.1.4)$$

and the corresponding energy is

$$E_n = \frac{\hbar^2 \pi^2}{2md^2} (n_x^2 + n_y^2) + \frac{\hbar^2 K_x^2}{2m} \quad (2.1.5)$$

2.1.3 Quantum wells (QW)

A physical situation that often arises in semiconductor devices is a carrier confined in one dimension, say Z to a thickness d and free in two dimensions say X and Y this is called 2D bands or quantum wells. In this case the solution of eq.(2.1.1) will have the form

$$\Psi_n(x, y, z) = \left(\frac{2}{d}\right)^{\frac{1}{2}} \sin \frac{n_z \pi z}{d} \exp(ik_x x) \exp(ik_y y) \quad (2.1.6)$$

and the energy of the carrier in the n^{th} band [6, 11] is

$$E_n = \frac{\hbar^2}{2md^2} n_z^2 + \frac{\hbar^2 k_x^2}{2m} + \frac{\hbar^2 k_y^2}{2m} \quad (2.1.7)$$

2.1.4 Density of state in low dimensional structures

An important manifestation of this sub band structure is the density of states (DOS) of electronic bands. The DOS figures importantly in both electrical and optical properties of any system. The density of state is the number of orbital per unit energy range. Therefore we can express the density of state for different quantum confinements as:

(i) For a bulk system $D(E) = \frac{dN}{dE}$ where $N = 2 \cdot \frac{4\pi K^3}{(2\pi)^3}$

$$D(E) = \frac{V}{2\pi^2} \left(\frac{2m}{\hbar^2}\right)^{\frac{3}{2}} E^{\frac{1}{2}} \quad (2.1.8)$$

(ii) For quantum well

- Conduction band

$$D(E) = \sum_i \frac{m^* \sigma(E - E_i)}{\pi \hbar^2} \quad (2.1.9)$$

where σ is heaviside step function $\sigma = 1$, if $E > E_i$, $\sigma = 0$ otherwise and E_i are the sub energy band levels

- Valence band

$$D(E) = \sum_i \sum_{j=1}^2 \frac{m^* \sigma(E_{ij} - E)}{\pi \hbar^2} \quad (2.1.10)$$

(iii) For quantum wire

$$N = \frac{KL}{\pi}$$

$$D(E) = \frac{1}{2\pi} \sqrt{\frac{2m}{\hbar^2}} E^{-\frac{1}{2}} \quad (2.1.11)$$

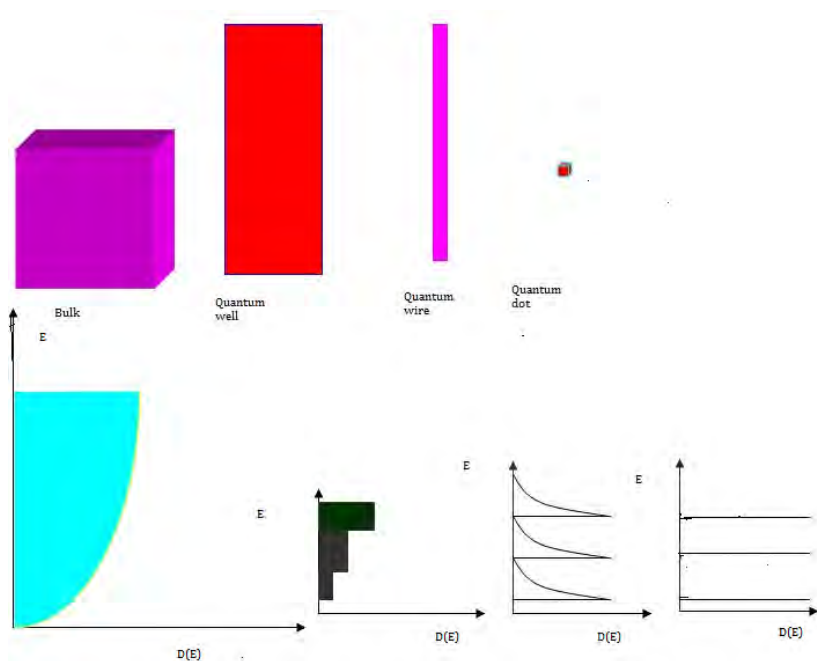


Figure 2.1: Change in density of state as the number of confining dimension increases

(iv) For quantum dot: The density of state is delta function.

$$D(E) = \delta(E - E_i) \quad (2.1.12)$$

2.2 Band structures of Si and Ge nanostructures

Luminescence is the emission of light by electrical or optical excitations. To get luminescence spectrum in the visible range the HOMO-LUMO gap has a great influence, which is related to the band gap energy of the bulk structure, there fore we need to study some of the methods for calculating band structures.

In semiconductors the Fermi energy lies in the gap between two bands, i.e there is an upper most completely filled band called valence band (VB), the unoccupied band is called the conduction band (CB), the two bands are separated by an energy gap E_g .

In fact nobody can tell either by experiment or calculations exactly what the upper edge of the conduction band looks like. The calculations need assumptions that might be enough to determine the band structure in the whole Brillouin zone. Here we present two standard methods for calculating band structures, the tight binding approximation and the pseudo potential method.

2.2.1 Tight binding approximations

This is also called the linear combination of atomic orbital (LCAO), in this approximation we assume that the valence wave functions of crystal atoms are slightly perturbed from their free state, and we limit on the nearest neighbor approximation and the most essential of the free atoms.

Si: $1s^2 2s^2 2p^6 3s^2 3p^2$

Ge: $1s^2 2s^2 2p^6 3s^2 3p^2 3d^{10} 4s^2 4p^2$

The valence electrons are made up of either s-type or p-type orbital. While this conclusion is strictly true for the elements in the atomic form, it turns out that even in the crystalline semiconductors the electrons in the valence and conduction band retains this s-type or p-type character even though they are "free" Bloch electrons.

The tight binding method (TBM) uses atomic functions as basis set for the Bloch functions. The periodic part of the Bloch function is represented by some combinations of atomic orbital centered at the lattice points.

If $\psi_n(r - R)$ represents such an orbital centered at R, we could write a Bloch function of the form:

$$\psi_k(r) = \sum_{R_n} \phi_n(r - R) \exp(ik \cdot R_n) \quad (2.2.1)$$

The periodic part of the Bloch function is expanded in terms of atomic-like orbital of the atoms of the unit cell.

The elements Si and Ge have valence electrons described by s-or p-type atomic orbital.

We assume the solution of the atomic problem

$$H_{at}\psi_n = E_n\psi_n \quad (2.2.2)$$

is already known for the atoms forming the crystalline material. This solution leads to the description of the electronic structure of various atoms. Constructing a Bloch state given by

$$\psi_k(r) = \sum_{n,R} \exp(ik.R)\psi_n(r - R_n) \quad (2.2.3)$$

But this state does not describe the new problem of the crystalline material where now we have

$$H_{cryst} = H_{at} + \Delta V(r) \quad (2.2.4)$$

where $\Delta V(r)$ is additional perturbation coming in due to interaction of neighboring atoms.

The new wave functions are now chosen as the more general wave functions

$$\psi_k(r) = \sum_R \exp(ik.R)\phi(r - R) \quad (2.2.5)$$

where $\phi(r)$ are not atomic functions, but can be constructed out of the atomic functions.

Expanding $\phi(r)$ in terms of atomic eigen functions $\psi_n(r)$ we have

$$\phi(r) = \sum_{n=1}^N b_n\psi_n(r) \quad (2.2.6)$$

The Schrodinger equation is now

$$H\psi_k = E(k)\psi_k \quad (2.2.7)$$

Using eqs.(2.2.5) and (2.2.6) for the eigen function ψ_k in eq.(2.2.7) and multiplying by $\psi_m^*(r)$ and integrating over space we get

$$\int d^3r \psi_m^*(r) [H_{at} + \Delta V(r)] \sum_{R,n} \exp(ik.R)\psi_n(r - R) = E(k) \sum_{R,n} \exp(ik.R) \quad (2.2.8)$$

Since the atomic wave functions are orthogonal we have

$$\int d^3r \psi_m^*(r) \psi_n(r) = \delta_{mn} \quad (2.2.9)$$

However the atomic wave functions centered at different sites are not orthogonal i.e

$$\int d^3r \psi_m^*(r) \psi_n(r - R) \neq \delta_{mn} \text{ for } R \neq 0$$

In the summation over lattice vectors we separate the terms $R = 0$ and $R \neq 0$ to get

$$\begin{aligned} (E(k) - E_m)b_m &= -(E(k) - E_m) \sum_{n=1}^N \left[\sum_{R \neq 0} \int d^3r \psi_m^*(r) \psi_n(r - R) \exp(ik \cdot R) \right] b_n \\ &+ \sum_{n=1}^N \left[\int d^3r \psi_m^*(r) \Delta V(r) \psi_n(r) \right] b_n \\ &+ \sum_{n=1}^N \left[\sum_{R \neq 0} \int d^3r \psi_m^*(r) \Delta V(r) \psi_n(r - R) \exp(ik \cdot R) \right] b_n \end{aligned} \quad (2.2.10)$$

where we have used

$$\int d^3r \psi_m^*(r) H_{at} \psi_n(r) = E_m \delta_{mn}$$

It can be pointed out that the atomic energies E_m may correspond to the isolated atomic energies. This is due to the modification arising from the neighboring atoms. We have an approximation

$$\int d^3r \psi_m^*(r) \psi_n(r - R) \exp(ik \cdot R) \approx 0$$

The approximation assumes that there is negligible overlap between neighboring atomic wave functions, i.e the atomic wave functions are tightly bound to the atoms.

$$\int d^3r \psi_m^*(r) H \psi_n(r) = E_m + \int d^3r \psi_m^*(r) \Delta V(r) \psi_n(r)$$

is called the on-site matrix element. For most potentials the on site integral

$$\int d^3r \psi_m^*(r) \Delta V(r) \psi_n(r) \approx 0 \text{ for } m \neq n$$

In semiconductors we have two atoms per basis and for each atom we need to include at least the outer shell s , p_x, p_y, p_z functions. Thus the secular equation of the tight binding quite difficult to solve.

To get some physical insight in to the problem consider a band structure arising from a single atomic s -level where $b_s=1$. In this case eq.(2.2.10) becomes

$$\begin{aligned}
(E(k) - E_s) &= -(E(k) - E_s) \sum_{R \neq 0} \int d^3r \psi_s^*(r) \psi_s(r - R) \exp(ik \cdot R) \\
&+ \int d^3r \psi_s^*(r) \Delta V(r) \psi_s(r) \\
&+ \sum_{R \neq 0} \int d^3r \psi_s^*(r) \Delta V(r) \psi_s(r - R) \exp(ik \cdot R)
\end{aligned} \tag{2.2.11}$$

Now let's denote

$$\begin{aligned}
\alpha(R) &= \int d^3r \psi_s^*(r) \psi_s(r - R) \\
\beta_s &= - \int d^3r \psi_s^*(r) \Delta V(r) \psi_s(r) \\
\gamma(R) &= - \int d^3r \psi_s^*(r) \Delta V(r) \psi_s(r - R)
\end{aligned}$$

from orthogonality $\alpha(R) = 0$, this gives

$$E = E_s - \beta_s - \sum_R \gamma(R) \exp(ik \cdot R) \tag{2.2.12}$$

The off-site integrals $\gamma(R)$ drop rapidly as the separation R increases [11].

2.2.2 The pseudo potential method (PPM)

The PPM is a powerful to solve for the band structure of semiconductors and often used as a bench mark for comparison of other techniques.

It makes use of information that the valence and conduction band states are orthogonal to the core states. The the back ground periodic potential is replaced by a new potential

that are softer than all electron potentials called "pseudo potential" which is obtained by subtracting out the effects of core levels. The pseudo potential includes relevant information to give the valence and conduction band structure. Here we seek a function which oscillates rapidly inside the core, but runs smoothly as a plane wave in the remainder of the open space.

Suppose we take

$$\psi_v(k, r) = \phi_v(k, r) - \sum_c \langle \psi_c | \psi_v \rangle \psi_c \quad (2.2.13)$$

The schrodinger equation for the valence and conduction band states is

$$\left[-\frac{\hbar^2}{2m}\nabla^2 + V(r)\right]\psi_v(k, r) = E_v\psi_v(k, r) \quad (2.2.14)$$

with the orthogonality condition $\langle \psi_c | \psi_v \rangle = 0$ where ψ_c are the core states

$$H\psi_v(k, r) = E_v\psi_v(k, r)$$

plugging eq.(2.2.13) in eq.(2.2.14) we have

$$H[\psi_v(k, r) - \sum_c \langle \psi_c | \psi_v \rangle \psi_c] = E_v[\psi_v - \sum_c \langle \psi_c | \psi_v \rangle \psi_c]$$

$$H\psi_v(k, r) - \sum_c [E_v(k) - E_c] \langle \psi_c | \psi_v \rangle \psi_c = E_v\psi_v(k, r)$$

where E_c is the core energy levels.

The Schrodinger equation $\psi_v(k, r)$ has the same eigen value as the original $\psi_v(k, r)$ together with the orthogonality condition, but with new back ground potential. The original potential $V(r)$ is replaced by the operator

$$V(r)\psi_v(k, r) \rightarrow V(r)\psi_v(k, r) + \sum_c [E_v(k) - E_c] \langle \psi_c | \psi_v \rangle \psi_c \quad (2.2.15)$$

Denoting $V_R = \sum_c [E_v(k) - E_c] \langle \psi_c | \psi_v \rangle$, we can write the effective potential as

$$V_P = V_R + V(r)$$

where $V(r)$ is the actual potential and V_P is the new potential operator which involves subtraction of the core energies weighted out with $\phi_v(k, r)$ from the eigen values $E_v(k)$ is called the pseudo potential.

The pseudo potential V_P is a non-localized eigen value dependant operator. The problem is simplified due to the realization that the pseudo potential is more smooth than the original starting potential. Since the term $-E_c < \psi_c | \psi_v >$ is a position term which subtracts the strong core effects near the atomic sites leaving the potential region between the atoms unchanged. The pseudo potential is thus equivalent to a constant

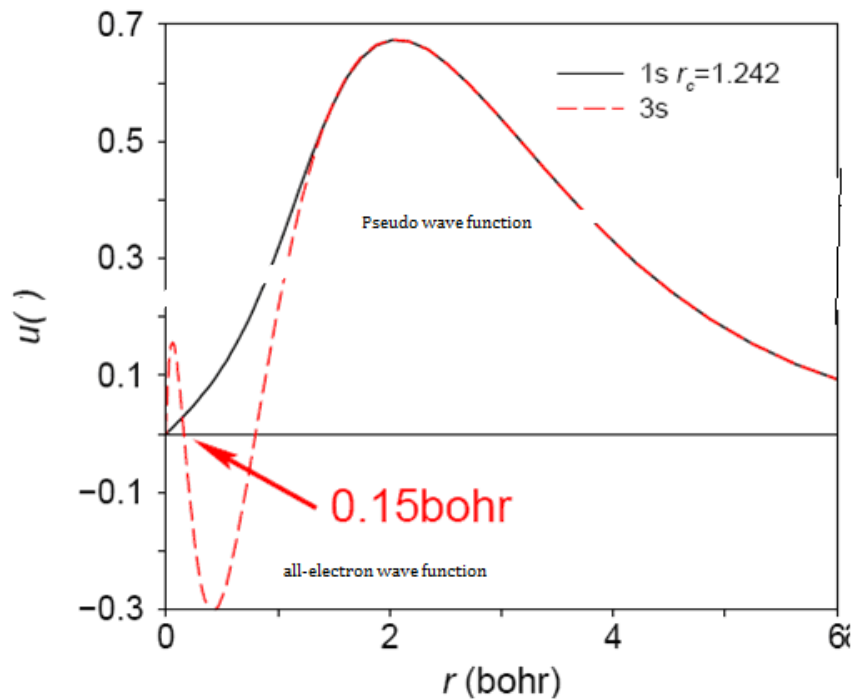


Figure 2.2: The actual potential and the pseudo potential with their corresponding wave functions [7]

potential plus a weak back-ground potential as far as the valence and conduction band states are concerned.

Since the valence energies lie above the core energies, the pseudo potential is positive so that $V(r) + V_P$ provides at least a partial cancelation to provide a weak enough potential

to do nearly free electron calculations for $\phi_v(k, r)$ (the so called pseudo wave function), treating the pseudo potential as a weak perturbations.

The pseudo potential for a problem is not unique nor exact, but it may be very good on the empty core model (ECM) we take the unscreened potential to be zero in side some radius R_e [13,14].

$$V(r) = 0, \text{ for } r < R_e$$

$$V(r) = -\frac{e^2}{r}, \text{ for } r > R_e$$

2.3 Excitons

Reflectance and absorption spectra often shows structure for photon energies just below the energy gap, where we might expect the crystal to be transparent. This structure is

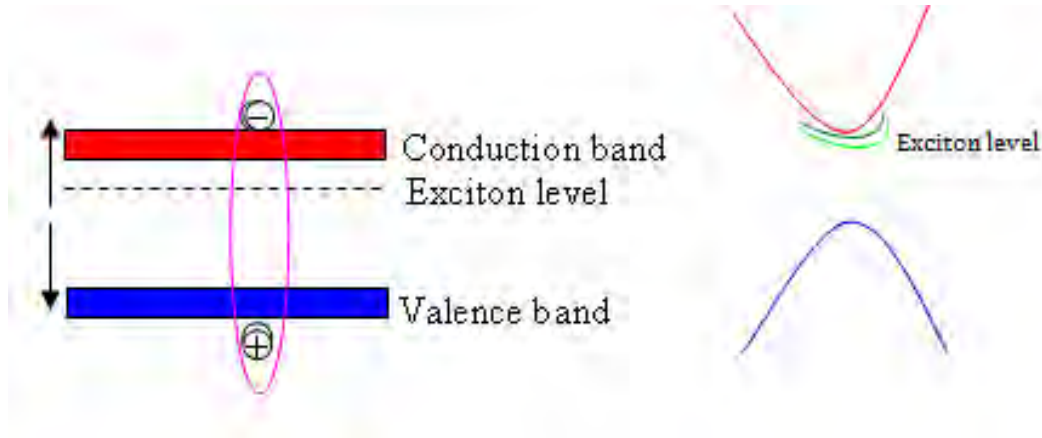


Figure 2.3: Exciton levels for transition from VB to CB [7]

just caused by the absorption of a photon with creation of a bound electron-hole pair. An electron and a hole may be bound together by their attractive coulomb interaction, just an electron is bound to a proton to form a neutral hydrogen atom. The bound electron-hole pair is called an exciton. An exciton can move through the crystal and transport energy; it does not transport charge because it is electrically neutral. Excitons can be formed in

every insulating crystal. When the band gap is indirect, excitons near the direct gap may be unstable with respect to the decay in to free electron and free hole. All excitons are unstable with respect to the ultimate recombination process in which electron drops in to the hole.

We have seen that a free electron and a free hole are created whenever a photon of energy greater than the energy gap is absorbed in a crystal. The threshold of this process is $\hbar\omega > E_g$ in a direct process. In an indirect process, the threshold is lower by the phonon energy $\hbar\Omega$. But in the formation of excitons the energy is lowered with respect to these thresholds by the binding energy of the exciton.

The binding energy of excitons can be measured in three ways:

- In optical transitions from the valence band, by the difference between the energy required to create an exciton and the energy to create a free electron and free hole.
- In recombination luminescence, by comparison of the energy of the free electron-hole pair recombination line with the energy of the exciton recombination line
- By photo-ionization of excitons, to form free carriers [7] .

In this chapter we have seen the general QC effects and the band structures of Si and Ge, the excitation of electrons from one energy level to the other; illumination can also give rises to new optical and electrical properties, so we need to study these properties.

Chapter 3

Optical and electrical properties of Si and Ge nanostructures

3.1 Porous silicon preparation

Porous silicon (P-Si) is generally prepared by anodization in a solution of hydrofluoric acid (HF) and ethanol. Using simple p-type or n-type wafers as a starting material. A strong photoluminescence (PL) can be achieved under optical excitations. However for strong electroluminescence (EL), it is necessary to create conditions for efficient carrier injection into the P-Si network; this can be achieved either by placing a metal contact in close to proximity of the P-Si layer or by forming a vertical p-n diode [15].

3.1.1 Emission and absorption of light

The emission and absorption of light in semiconductors is very analogous to the same process that we quite familiar with in atoms, an electron in an excited state of energy E_1 makes a transition downwards to an empty state (energy E_0) and emits a photon; an electron in a lower state (energy E_0) absorbs a photon and makes a transition to higher state (energy E_1). The energy conservation equation is $E_{photon} = \hbar\omega = \Delta E_{electron} = E_1 - E_0$.

The band gap of insulators is what makes them relatively transparent if the incoming

light has a frequency $\omega < \frac{E_g}{\hbar}$, then it cannot be absorbed by the electrons filling the valence band. The very low absorption of wide-gap insulators is generally due to impurities, so light penetrates relatively deeply into them [16].

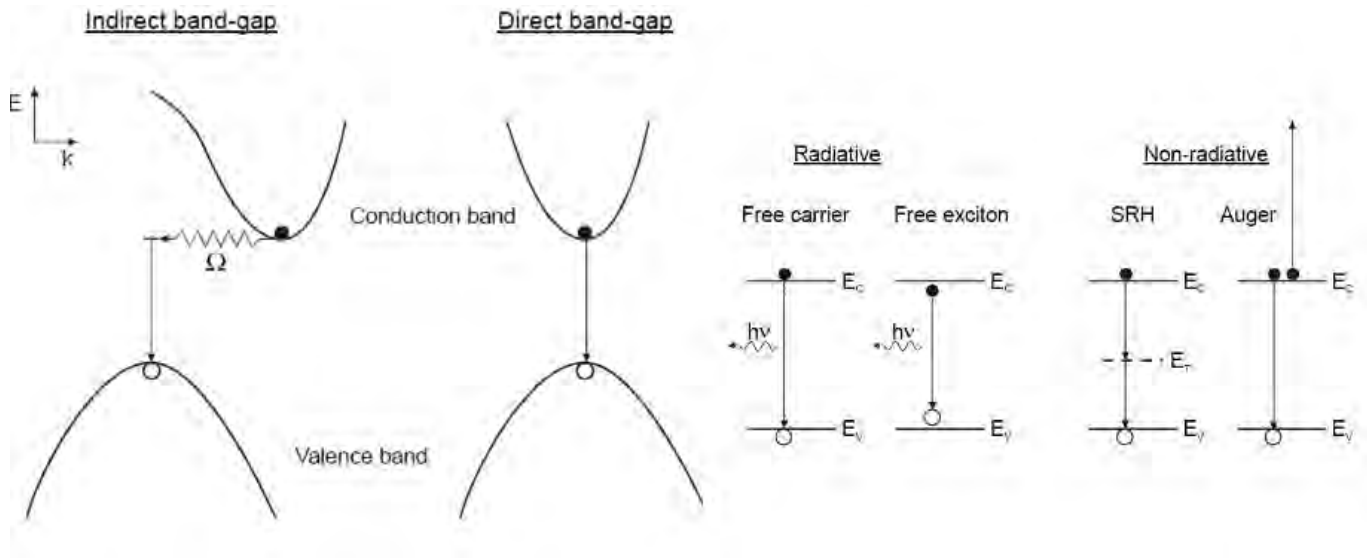


Figure 3.1: Direct and indirect band transitions [15]

Besides to Si and Ge, most semiconductors are in fact indirect band gap materials. The band structure of a material is intimately dependent on several factors, including crystal structure, lattice constant, chemical species, bond length, electronegativity, stiffness and elasticity.

Conventionally the band structure of a semiconductor is represented by the dispersion relation $E_n(k)$ where E is the energy of an electron (or a hole) at the band edge with a wave vector \mathbf{k} in the first Brillouin zone. The indirect gap also affects absorption of incident radiation. Photoexcitation of carriers can occur both by absorption or emission of phonons in indirect semiconductors. The absorption coefficient α has a quadratic dependence on a photon energy and has two branches.

In direct semiconductors no phonon assistance is needed and α shows a parabolic dependence with incident photon energy. The net result is that when band-to-band absorption occurs in direct semiconductors, the incident radiation is absorbed in a much

shallower depth than in an indirect semiconductors the forbidden gap can also mediate an electron-hole pair recombination. In an indirect semiconductors, a phonon assistance may still be required making gap state mediated radiative recombination potentially less efficient than a direct transition [17].

3.2 Luminescence

Luminescence is light that usually occurs at low temperature and thus form a cold body radiation, which distinguishes it from incandescence. It is a general term which describes any process in which energy is emitted from a material at different wavelengths [18].

Opto-electronic devices work by exciting electron-hole pairs; when a pair recombines it emits light. This is called luminescence. It results when there is a significant overlap (indirect and reciprocal space) in the electron-hole pair wave functions. Whenever there is such overlap, luminescence is possible; however the strength of the luminescence, that is light emission rate and quantum efficiency depend on the extent of this overlap and the transition probability [17].

There are different types of luminescence; here we mention photoluminescence and electroluminescence. Electroluminescence is the excitation of carriers by electrical current or strong electric field, often practical method; and photoluminescence is the excitation of carriers by light it self, it is usually caused by optical radiation [16,18].

Luminescence is further broken down into two categories according to the speed of recombination. Direct electron-hole recombination is usually relatively fast: the lifetime depends on the number of final states available.

The excited electron first makes a transition to such a state, whose energy normally lies in the gap. Then it makes a second transition to finally recombine with the hole in the valence band. Often one of these transitions is non-radiative, by this it meant that the energy given off in the transition appears as heat, not light.

3.2.1 Recombination rates

The recombination rate for electron hole pairs is given by

$$\frac{dN(t)}{dt} = -\alpha_r N(t)P(t)$$

$N(t)$ is the number of electrons and $P(t)$ is the number of holes, α_r is a constant that we could calculate, given our knowledge of transitions between quantum states. It is an integral involving the electric field, and the initial and final state wave functions.

In addition to this there is a thermal generation rate for e-h pairs.

$$\left[\frac{dN(t)}{dt}\right]_{thermal} = \alpha_r N_i^2$$

Now let us say that we are in thermal equilibrium in an intrinsic semiconductor. This is a steady state, and $N(t)=P(t)$ so

$$\left[\frac{dN(t)}{dt}\right]_{total} = \alpha_r N_i^2 - \alpha_r N(t)P(t) = \alpha_r [N_i^2 - N^2(t)]$$

$N(t) = N_i$, a constant. Thus N_i has the meaning of the number of carriers in an intrinsic semiconductor in thermal equilibrium. It is a strong function of temperature. In thermal equilibrium in general, we have

$$\left[\frac{dN(t)}{dt}\right]_{total} = \alpha_r N_i^2 - \alpha_r N(t)P(t) = 0$$

So $N(t) P(t)=N_i^2$; the product of electron and hole concentrations (in equilibrium) is always the same, it does not depend on doping, which is somewhat surprising. Note that in an n-type material, we would have $N(t) \gg P(t)$, and vice-versa for a p-type.

Now let us think about a situation where we shine a pulse of light on a p-type sample. $N(0)$ will depend on the strength of the pulse, and then it will relax back to its equilibrium value $N_c = \frac{N_i^2}{N_v}$. We have $N(t) \ll P(t)$, but $P(t)$ is not much changed from its base value, so let $P(t)=N_v$

$$N(t) = N_c + [N_0 - N_c] \exp \frac{-t}{\tau}$$

where $\tau = \frac{1}{\alpha_r N_v}$ for p-type, and $\tau = \frac{1}{\alpha_r N_c}$ for n-type [16].

3.3 Photoluminescence

Luminescence resulting from optical excitation is called photoluminescence (PL). Typically for Si nanocrystal (Si-nc) PL extends from 600 nm to 1000 nm [19]. The excitation source is laser with photon energy larger than band gap energy E_g . Electrons and holes relax rapidly by interacting with photon or phonon with lattice vibrations \rightarrow electrons \rightarrow phonon coupling ~ 100 fs: much faster than the radiative life time.

PL reaches thermal distribution according to Fermi-Dirac distribution, photon emission from E_g

$$f(E) = \frac{1}{\exp\left(\frac{E-\mu}{K_B T}\right) + 1} \quad (3.3.1)$$

The concentration of electrons in the conduction band is [7].

$$n(T) = \int_{E_g}^{\infty} D_c(E) f_e(E) dE \quad (3.3.2)$$

$$n(T) = \frac{1}{2\pi^2} \left(\frac{2m_e^*}{\hbar^2}\right)^{\frac{3}{2}} \int_0^{\infty} E^{\frac{1}{2}} \left[1 + \exp\left(\frac{E-\mu}{K_B T}\right)\right]^{-1} dE \quad (3.3.3)$$

and the concentration of holes in the valence band is:

$$p(T) = \int_{-\infty}^{E_v} D_v(E) f_h(E) dE \quad (3.3.4)$$

$$p(T) = \frac{1}{2\pi^2} \left(\frac{2m_h^*}{\hbar^2}\right)^{\frac{3}{2}} \int_{-\infty}^0 E^{\frac{1}{2}} \left[1 + \exp\left(\frac{\mu - E}{K_B T}\right)\right]^{-1} dE \quad (3.3.5)$$

3.3.1 The photoluminescence of porous silicon

The photoluminescence from P-Si is at wavelength ranging from the ultraviolet to the infrared [20]. The PL is usually excited by a wavelength shorter than the emission wavelength with excitation wavelengths typically lying between 260 nm (for ultraviolet emission) and approximately 520 nm [4]. Alternatively PL can be excited through an up conversation process by pumping the P-Si at the infrared wavelengths [21,22].

The characteristics of PL changes as the wavelength of emission changes from ultraviolet wavelengths to infrared wavelengths. A Specific characteristics normally applied to a

discrete set of wavelengths in to three bands to describe these characteristics. The main characteristics of each of wavelength bands called the 'red', 'blue', and 'infrared' bands.

Normally it is very difficult to compare one's own result of luminescence investigations with those of another authors due to the use of relative units for intensity. To overcome this problem, integral features of spectra such as peak areas can be given in terms of an efficiency. The spectra shown in this work are mapped on an energy scale, and there fore a peak area is proportional to the emitted energy, not to the number of emitted photons. The efficiency η_p is defined as the ratio of the light out put power to the in put power, which is the light in put power in the case of PL or electrical out put power in the case of EL.

In the literature terms the external quantum efficiency η_E or internal quantum efficiency η_I are often used. Here by η_E is defined as the ratio of the number of emitted photons to the number of incident photons (electrons), where as η_I is the ratio of the number of emitted photon to the number of photons directly absorbed by the luminescence centers. These efficiencies fulfill the equation $\eta_p < \eta_E < \eta_I$. In the PL η_p and η_E differ by of the energy of exciting to the emitted photons and both are similarly suitable to characterize the achieved intensity. However in the case of EL and high applied voltages the use of η_E could give rise to misunderstandings [23].

3.4 Electroluminescence

Electroluminescence is an optical and electrical phenomenon in which materials emit light in response to an electric current through it, or to a strong electric field. It is the result of radiative recombination of electrons and holes in a material (usually semiconductors) luminescent device such as light emitting diodes (LEDs), or through excitation by impact of high energy electrons accelerated by strong electric field (as with phosphorus in electroluminescent display).

3.4.1 Practical applications

The most common EL devices are either powder (primarily used in lightening applications or in thin films) for information displays. Electroluminescent automotive instruments panel back lightening with each gauge pointer also an individual light source. Electroluminescent technologies have low power consumption compared to the competing light technologies, such as neon or fluorescent lamps. This together with the thinness of the

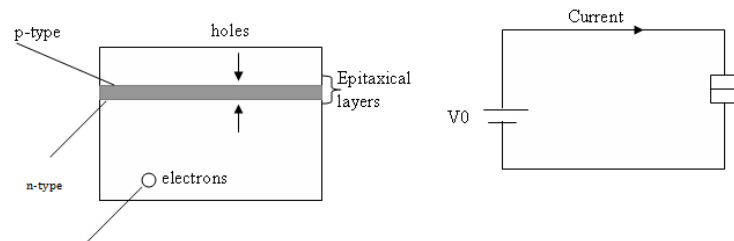


Figure 3.2: Electron -hole structures in semiconductors [25]

material has made EL technology valuable to the advertising industry. EL manufacturers are able to control precisely which areas of electroluminescent sheet illuminate and when.

In principle EL lamps can be made in any color. However, the commonly used greenish color precisely matches with peak sensitivity of human vision producing the greatest apparent light out put for the least electrical power in put. Unlike neon the fluorescent

lamps, EL not negative resistance devices so extra circuitry is needed to regulate the amount of current flowing through them [24].

The excitation source of EL is electrical current through optoelectronic devices, light emitting diodes and laser diodes. Microscopic EL mechanism is the same as PL. At room temperature a single light emission line of width $\sim K_B T$ at the band edge E_g is expected. Factors that affect the EL are:

- The size of the band gap.
- Constraint relating the lattice matching.
- The ease of p-type doping

3.4.2 Types of electroluminescence

Basically we have two types of electroluminescence; high field EL and injection EL. In injection EL light is emitted up on recombination of minority and majority carriers across the band gaps and high luminescence efficiency through out the visible region of the spectrum.

Two more phenomena i.e photoelectroluminescence(PEL) and electrophotoluminescence(EPL) are also used nowadays. PEL is used whenever the excitation mechanism of the electric field is influenced by additional irradiation and EPL is the term employed when the luminescence by irradiation (with UV, X-rays, cathode rays etc) is controlled by electric fields, leading to the enhancement or to a quenching effect of the luminescence emission. This is generally termed as Gudden-Pohl effect. The main difference between EPL and EL is that the EPL is an empty of traps by electric field where as the EL is the field of excitation of the luminescence centers.

3.4.3 Fundamental physical processes

There are four fundamental process in EL behavior which may lead to light emission.

These processes are.

- (i) Injection of charge carrier in to phosphor layers.
- (ii) Acceleration of charge carriers to optical energies.
- (iii) Excitation luminescence centers by energetic electrons (impact excitation)and
- (iv) Radiative relaxation of luminescence centers.

3.4.4 Injection electroluminescence

In 1952 Haynes and Briggs first reported the infrared EL from a forward biased p-n junction (or through rectifying contact on a crystal) is termed an injection "EL". These diodes are usually called light emitting diodes and have been widely used since late 1960's. Semiconductors with a wide band gap show this type of EL.

The mechanism of light generation in injection EL and high field EL are quite different from each other. There are two methods with which injection of minority carriers can occur. In the first method the injection occurs from an electrode (rectifying contact) in to the crystal. The electrons are accelerated and excite the luminescence centers similar to the case of high field EL. Only the source of electrons is different. This type of injection EL can be observed in single crystals of Zinc sulfide or in thin films that have contact with electrodes.

In the second method, light emission occurs at a p-n junction. At thermal equilibrium, a depletion layer is formed and diffusion potential V_d across the junction is produced. When the p-n junction is forward biased, the diffusion potential decreases to $(V_d - V)$ and electrons are injected from the p-region to the n-region; i.e minority carriers injection takes place. Subsequently, the minority carriers diffuse and recombine with majority carriers directly or through trapping at various kinds of recombination centers producing

injection EL.

The following relation gives the total diffusion current on a p-n junction.

$$J = J_h + J_e + J_s[\exp(\frac{qV}{nKT}) - 1] \quad (3.4.1)$$

$$J_s = q(\frac{D_h p}{L_h} + \frac{D_e n}{L_e}) \quad (3.4.2)$$

where D_h and D_e are diffusion coefficients for holes and electrons, p and n are the concentrations of holes and electrons respectively as minority carriers at thermal equilibrium, and L_h and L_e are diffusion lengths of holes and electrons respectively which is given by $(D\tau)^{0.5}$ where τ is the life time of minority carriers [25].

In this chapter we have studied, the optical and electrical properties of pure Si and Ge nanostructures like EL and PL, when these materials are terminated with oxygen and hydrogen, the band gap increases and acquires its own properties; which leads to another explanation to study EL and PL for such structures.

Chapter 4

Luminescence through impurities in Si and Ge nanostructures

4.1 Introduction

In this chapter the PL and EL of Si and Ge passivated with oxygen (O) and hydrogen (H) are presented, but due to its wide applications attention is given to the EL of Si embedded in SiO₂ matrix.

Electron-hole pairs injected electronically or optically can recombine through impurity centers with enhanced recombination rates compared to that of pure Si crystal, where recombination is intrinsically very low. The enhancement, in a simplified manner can be considered as a consequence of relaxed \mathbf{k} -selection (momentum conservation) requirement due to the localization of electron hole pairs near impurity centers. The detailed process depend on the properties such as the symmetry of impurity state with respect to that of the wave functions of electrons in the CB and the holes in the VB, the degree of localization and so on, of the specific impurity center. The energy from the recombination of an e-h pair can be released by generating a photon or a phonon, or phonons, or through a variety of other channels. Each of these channels has certain probability and the one that has the highest probability dominates the nature of a given impurity center. For example the centers for which the dominant energy release channel is the emission of a photon customarily termed "radiative impurity center", where as those for which the dominant

energy release channels are phonon emission, Auger process and so forth, are termed as "non-radiative impurity centers." In Si, the recombination of e-h pairs through impurity centers is in general non-radiative.

4.2 Silicon nanocrystals in SiO₂

While P-Si exhibit luminescence properties, its stability was a deriving force for the investigation of other structures, where Si nanocrystals would be better passivated. By forming Si nanocrystals within SiO₂, the unstable H₂ would be replaced by SiO₂. One way to form Si nanocrystals embedded in SiO₂ is to create an excess Si concentration in the oxide by Si implantation and to induce nanocrystal formation and growth by subsequent high temperature annealing [15].

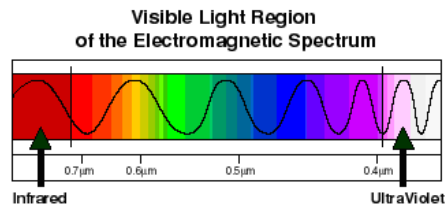


Figure 4.1: Visible light spectrum [39]

The optimum passivation time that varies with the quality of SiO₂ (fused silica, wet and dry SiO₂ grown process) and the Si implantation depth profile. The effect of passivation on time for the SiO₂ samples implanted with Si ions varies with energy. Passivation can also induce a blue shift or a red shift of the PL spectrum. The PL spectrum has been red shifted after passivation of the sample implanted to high excess Si concentration, while no spectrum shift has been observed at low excess Si concentration. On the other hand the PL intensity decreases (increases) with a red shift (blue shift) of the PL spectrum.

Color	wavelength(nm)
Red	625-740
Orange	590-625
Yellow	555-590
Green	520-555
Cyan	500-520
Blue	435-500
Violet	380-435

When a larger concentration of Si is implanted, the luminescence signal decreases with the Si concentration. However the effects of Si-nc size, shape and distribution on the PL spectra remains complex due to the presence of several radiative transition process [19]. Si/SiO₂ interface is one of the most studied interface because of technological importance

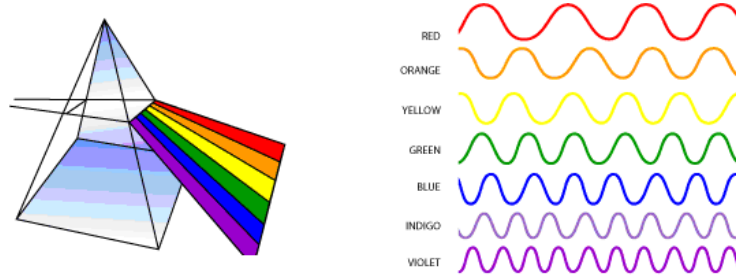


Figure 4.2: Different wavelength of electromagnetic spectrum [39]

of thin SiO₂ films in semiconductor devices. Gate dielectrics, mask layers, insulators etc.

Many different investigations have shown that a flat interface between Si and SiO₂ is formed, this extremely sharp (at single atom level) and extremely stable with the external agents. For this reason Si-nc embedded in a SiO₂ matrix have been used to form light emitting systems with superior properties with respect to P-Si which is formed by Si nanostructures with time dependant surface passivation. The quality and stability of the Si/SiO₂ interface in Si-nc embedded in SiO₂ is what renders this system superior.

The role of the interface on the electronic and optical properties of Si-nc has been

recently addressed in various experimental and theoretical studies. The oxidation introduces defect levels in the Si-nc band-gap which pin their emission energy. The defect levels are due to the formation of Si-O double bond. Similar results can be obtained also for O connecting two Si atoms (single bond) at the Si-nc surface the assistance of Si-O vibrations at the interface has been proposed the dominant path for recombination [26].

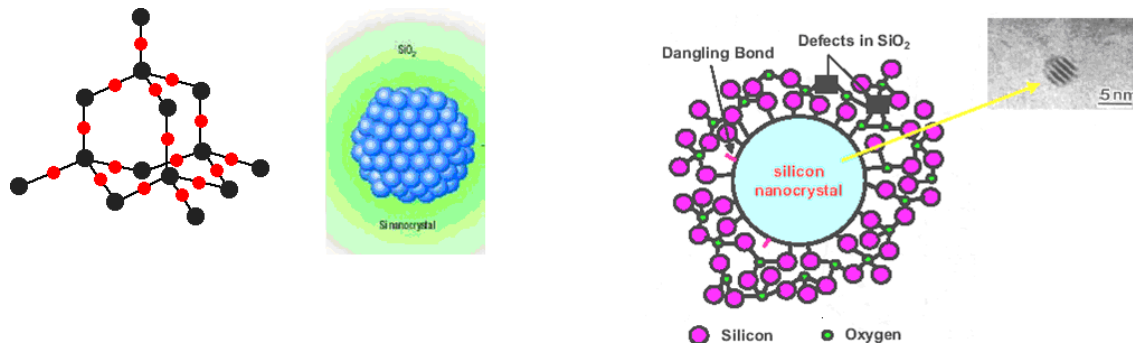


Figure 4.3: Bond structures of Si and O [26, 41,42]

Si-ncs embedded in a SiO_2 matrix are currently attracting great interest as a candidate system to solve the physical inability of the bulk Si, due to its indirect energy band gap, to act as an efficient light emitter; the emission is shifted in the visible region due to QC effects. The radiative recombination of e-h pairs generated inside a nanocrystal embedded in SiO_2 is also very efficient at room temperature. Amorphous Si nanoclusters have also received considerable attention as light emitting material. The electrical properties are strictly related to the peculiar structure of the active layer, consisting of a very high density of partially interconnected and very small amorphous clusters. Due to a strong dependence of current, the electronic conduction cannot be explained by a model based on tunneling mechanisms [27].

EL is a very important feature for any long optoelectronic technology. Its characterization and optimization are essential for the development of all Si light emitting diodes (LEDs) and eventually of a Si laser. EL has been first reported in amorphous Si because of the difficulty of electrical pumping of the Si-nc embedded in an insulating matrix

(SiO₂). However when SiO₂ is thin enough and appropriate set up is used, EL can also be observed in Si-nc produced by ion implantation and plasma enhanced chemical vapor deposition PECVD with low activation voltage.

The electrical carrier injection is usually performed by means of a structure resembling metal-oxide-semiconductor (MOS) device. Transparent thin electrodes are deposited on to the Si-nc/SiO₂ layer. The size of this electrode is kept small to concentrate the injected electrons [19].

Si nanocluster embedded in a SiO₂ matrices hinder the attainability of stable efficient electrically driven light emitting devices owing to a huge barrier mismatch between Si and SiO₂. The EL emission crystalline Si nanoclusters must be grown or past-annealed at high temperature to participate the crystalline Si nanoclusters. The PL peak energy as a function of diameter of Si nanoclusters can be obtained by fitting the relation ship between PL peak energy and diameter of Si nanoclusters, the dependence of the associated energy-gap E (eV) on the diameter d (nm) of the Si nanoclusters can be expressed as [28, 29].

$$E(eV) = 1.17 + \frac{11.6}{d^2} \quad (4.2.1)$$

Eq.(4.2.1) can be substituted in the QC model to get the luminescence intensity.

4.3 EL signal enhancement by hydrogen passivation

Hydrogen is usually a component of acids or gases used for the production of Si-nc by means of electrochemistry process film deposition. On the other hand Si ion implantation can be generated in different defects in SiO₂ layer. Defects are also observed in oxidized amorphous Si films deposited by PECVD. Annealing at high temperature ($\sim 1000^0c$) causes the nucleation and growth of Si-nc and eliminate most of the defects. However, it has been shown that passivation ($\sim 500^0c$) in an environment containing H increases the luminescence by as much as one order of magnitude. Many studies related that this strong increase in the luminescence to termination by H of dangling bonds responsible for non-radiative recombination. H is mobile at temperatures greater than $\sim 400^0c$, but diffuses at $\sim 600^0c$ with an accompanying decrease of the PL or EL intensity. Thus a two step process (anneal at 1100^0c and passivation at 500^0c) achieves a better luminescence quality than the one step anneal and passivation both at 1100^0c [19].

This section presents the analysis of hydrogenated silicon nanoclusters (H-Si-nc). The aim is to investigate the structural, electronic and stability of H-passivated Si-nc as a function of both size and symmetry as well as pointing out the main changes induced by the nanocrystal excitation.

The nanocluster excitation has been studied calculating pair excitation energies. The formation of e-h pair under excitation is taken in to account for one electron occupy the LUMO, thus leaving a hole in the HOMO. Thus the nanocluster excitation occurs with atomic positions fixed in their ground state configurations, we indicate that $E(N, e-h)$ the total energy of the nanocrystal calculated with the e-h pair. The difference $E_{ex}^A = E(N, e-h) - E(N)$; ($E(N)$ being the N-electron ground state total energy) gives the energy needed for the creation of the pair, and defines the absorption edge.

$E(N) = E_1$ and $E(N, e-h) = E_2$; E_1 and E_2 being the cluster total energies. It should be noted that the quasi-particle gap defined as $E(N+1) + E(N-1) - 2E(N)$, and calculated from N+1,

N-1 and N electron total energies, neglect the effect of the coulomb attraction between electron and the hole; actually this gap is calculated starting from the energies needed the creation of a hole and one electron separately.

After excitation, due to the change in the charge density, relaxation occurs until the atoms reach a new minimum energy configuration, in the presence of e-h pair. This modifies the electronic spectrum, imply that levels involved in the emission process (e-h pair recombination) change.

The emission energy can be defined as $E_{ex}^E = E'(N, e-h) - E'(N)$ where $E'(N, e-h)$ and $E'(N)$ are the nanocluster total energies evaluated in the presence and absence of e-h pairs respectively, with atoms occupying the equilibrium position of the excited state with $E'(N, e-h) = E_3$ and $E'(N) = E_4$.

There are two interesting points which worth stressing here. The first one concerns the way in which the ground state structural properties change as a function of the cluster dimension, while the second is related to how creation of an e-h pair modifies the over all structures.

The Si-H bond lengths remain practically unchanged for both the ground and excited state configurations in contrast with Si-Si distances (indicating that the excitation concerns the Si shells rather than being simply localized on the surface).

The presence of an e-h pair in the clusters causes a strong deformation of the structures with respect to their ground state configuration and this is more evident for smaller systems. This is what we expect, since for large clusters the charge density perturbation is distributed through out the structure, and the effect locally induced becomes less evident.

(i) The ground state energy gap decreases on increasing the cluster dimension as expected.
(ii) The excitation of e-h pair causes a reduction of the energy gap which is more significant for smaller clusters. The smaller the H-Si-nc, the longer the difference between the absorption and HOMO-LUMO ground state-gap and between emission and HOMO-LUMO excited state gap [30, 31].

4.4 Electroluminescence and photoluminescence of Ge-implanted Si/SiO₂ and Si structures

The observation of efficient PL in P-Si has promoted numerous investigations of optoelectronic properties of nanometer-scale group IV semiconductor clusters. EL has been reported for P-Si during anodic oxidation. Although P-Si has motivated considerable interest in nanocrystalline semiconductors, there is interest in other related materials which are more robust in various thermal and chemical ambient and which can readily incorporated in to Si integrated circuit process, or on to substrates other than single crystal Si with out significant modification of the circuit process technology.

A number of alternative synthesis approaches have been reported, ranging from

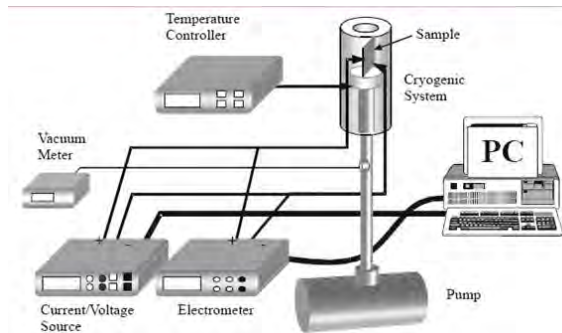


Figure 4.4: Device set up for electroluminescence measurements [40]

synthesis of nanocrystals inorganic solutions from chemical precursors to nanocrystals embedded in an oxide matrix prepared by consputtering or ion implantation. The latter approach is quite promising, owing to both mechanical and chemical robustness of the matrix, as one may expect the nanocrystal-matrix interface to be well passivated from the external ambient, and thus ultimately enabling better control of non-radiative recombination processes which limit luminescence. In addition the prospects for integration of these materials into existing Si based solid state devices and circuits is excellent.

4.5 Transmission measurement of EL

The absorption coefficient α is defined by:

$$I(x) = I_0 \exp(-\alpha x) \quad (4.5.1)$$

where I_0 and I are the intensities of the incident light before and after it passes the sample and x is the effective thickness of the sample. By measuring I , I_0 and x , we can determine α . The attenuation in I is not only by the absorption in the material but also by scattering at inner surface of voids in P-Si.

The intensity of EL signal is related to α through

$$I_{EL} = QI_0[1 - \exp(-\alpha x)] \quad (4.5.2)$$

where Q is the total conversion factor which can be affected by reflectivity, quantum efficiency of the luminescence, geometry factors etc.

Can constricted wires show EL?

For EL P-Si which allows higher current densities than non-electroluminescent, we assume that the current flows through the constricted wires where only constrictions are thin enough to act as quantum barriers. For PL such a structure is in active because the excited charges can move the low gap regions. However if a current flows through the wire, the charges are forced to pass a high gap regions. We want to give the argument that the constriction might be important for EL. It seems probable that the constricted regions with a high effective gap play the potential part for EL. An argument against the above discussion could be a large voltage drop over the constriction, for example if these regions have a lower dielectric constant(ϵ), in this case we have to argue that we also expect there a low mobility of charges, thus increasing the dwell time in the high gap region. Surface states which are proposed to play an important role for luminescence of Si-nc could even more cause the charges to stick a high gap regions [32].

4.6 Dependence of EL intensity on temperature

EL in 3D Si/SiGe nanostructures was found almost simultaneously with in the first investigation of the PL. In many of the Si-based nanostructures with promising PL properties like Si nanocrystals embedded in SiO₂, it is difficult to obtain due to poor carrier transport. In contrast, vertical carrier transport in Si/SiGe multi layers and 3D Si/SiGe nanostructures (NSs) is very efficient, and a simple device where Si/SiGe multi layers are embedded

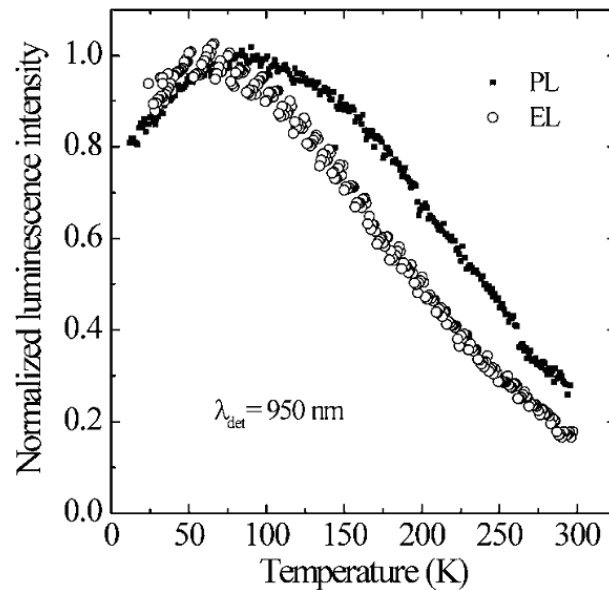


Figure 4.5: EL and PL intensities measured at 950 nm as a function of temperature. The EL intensity is measured with current density of 0.16 A/cm² and the PL intensity with a 488 nm pump laser power of 10 mW [34]

in to a p-n diode or similar structure can easily be fabricated. The measured EL spectrum is broad with a symmetric spectral shape, which is similar to the PL spectra, can be well fitted by two Gaussian bands separated by ~ 45 meV. This separation energy is close to SiGe characteristic phonon energy, proving that the EL mechanism is nearly identical to the PL one, that it is due to radiative e-h recombination in 3D Si/SiGe layered NSs. On increasing applied voltage, we can observe (similar to that in PL spectra under increasing photo excitation intensity) a noticeable EL spectra shift toward greater photon energies,

that is a "blue shifted". EL intensity as a function of temperature with its initial value I_0 can be fitted by a standard equation:

$$I_{EL}(T) = \frac{I_0}{1 + C_1 \exp \frac{-E_1}{K_B T} + C_2 \exp \frac{-E_2}{K_B T}} \quad (4.6.1)$$

with two thermal quenching activation energies E_1 and E_2 . Here T is the temperature and K_B is the Boltzmann constant, C_1 and C_2 are scaling coefficients. The EL thermal quenching activation energy $\simeq 130$ meV. Interestingly, in the sample, the device current as a function of temperature depicts nearly exact anti-correlation with the EL intensity and exhibits an activation energy of ~ 140 meV. The activation energy E_1 is independent of the intensity, while E_2 depends significantly on the excitation intensity [33].

4.6.1 Temperature Dependence of EL for Si impurities

Si nanocrystals embedded in a SiO_2 matrix are currently attracting great interest as a candidate system to solve the physical inability of bulk Si, due to its indirect band gap to act as an efficient light emitter. In deed the process of radiative recombination of e-h pairs generated inside a Si-nc embedded in a SiO_2 is also a very efficient at room temperature. Further more, since the band gap of Si-nc is enlarged with respect to the bulk material due to QC effects, the emission is shifted to the visible region. Amorphous Si-nanoclusters have also received considerable attention as light emitting material.

The electrical properties are strictly related to the peculiar structure of the active layer, consisting of a very high density of partially interconnected and very small amorphous clusters.

Due to strong dependence of current, the electron conduction can not be completely explained by a model based on tunneling mechanisms such as direct tunneling. The voltage dependence and temperature behavior indicate that the electrical conduction can be ascribed based on the emission trapped electrons towards the dielectric conduction band at a high electric field values. The well known equation which models this process

is:

$$J = A.\varepsilon. \exp\left(\frac{-\phi_t - \gamma\sqrt{\varepsilon}}{\frac{K_B T}{q}}\right) \quad (4.6.2)$$

where J is the current density, A is a proportionality constant, ε is the electric field, q is the electric charge, K_B is the Boltzmann constant, T is the absolute temperature, ϕ_t is the potential barrier at the trap/dielectric interface (at zero field), and $\gamma = \sqrt{\frac{q}{\pi\epsilon_0\epsilon_r}}$ the coefficient regulating the field induced barrier lowering; where as ϵ_0 , and ϵ_r are the absolute and relative dielectric constants respectively ($\epsilon_r=4$) only at high fields [34].

4.7 Transient properties of EL and its degradation

To investigate the carrier injection and relevant carrier recombination mechanisms, time resolved measurements of the EL have been generated by spectrally resolved EL decays, a stretch exponential dependence, which can be described by the function:

$$I(t) = I_0 \exp\left(\frac{-t}{\tau}\right)^\beta \quad (4.7.1)$$

where the decay is described by a time constant τ , the EL life time taken to be 2 to 60 μs for 3.4 nm dot with increasing wavelength and the dispersion factor β ($0 < \beta < 1$). $\beta=0.6$ for 3.4 nm dot and $\beta=0.54$ for 4.2 nm dot. In the case of single exponential decay (as for a homogeneous system of luminescent centra) $\beta=1$. If the decay consists of a combinations of several exponential reflecting a dispersion in life times for the same observation wavelength, then the value of β is less than 1 and decay is faster in the beginning. Several possible origins of this dispersion have been suggested for P-Si. The values of τ and β were found to be similar for the EL and PL from similarly prepared samples, indicating that the same luminescence mechanism is responsible for both EL and PL.

4.7.1 Electroluminescence degradation

Basically we have two types of EL degradation; reversible and irreversible (permanent) degradations. When a constant bias is applied to P-Si diodes, the EL intensity and current

remains constant for a short time ($\leq 1\text{ms}$) and decrease with time constants in the order of $\sim 100\text{ms}$. The degradation is partially reversible and depends on the pulse current and duration. At a low operating power recovery is complete and there is no spectral shift, indicating no structural changes in the P-Si network. The recovery time constant at room temperature are in the range of tens of seconds, but decrease rapidly with increase of temperature. By generating data with the expression:

$$\tau_r^{-1} = \tau_0^{-1} \exp \frac{-E_a}{K_B T} \quad (4.7.2)$$

as for a thermally activated recovery process, we can determine the activation energy E_a . This was attributed to the thermally activated release of trapped energy carriers from larger crystallites with lower band gap. Thus the reversible EL degradation has been attributed to a charging mechanism in the P-Si network and we propose that it might be assigned to coulomb blockade, caused by the trapping of carriers at larger crystallites with lower band-gap inhibiting further injection of carriers in to luminescent crystallites. This interpretation, rather than a mechanism of transient change of passivation, is supported by a concurrent reduction of the injected current (at a fixed voltage). Since the recovery process is two orders of magnitude slower than the degradation, a lowering operational duty-cycle is a serious limitation for potential applications of these LEDs.

Only part of the degradation of the EL from the P-Si LEDs is recoverable. A permanent degradation takes place during the operation as well. One of the possible reason for the degradation is a local heating in the region of a high porosity, due to a low heat conductivity. The heating causes deterioration of the surface passivation through stimulated hydrogen desorption, and thus increases the non-radiative recombination [15, 28, 29].

In the previous chapters, we have seen the existing theories and explanations on the features of Si and Ge nanostructures in general, and the EL and PL spectrum in particular. Now we have to formulate models to study PL and EL intensities for these structures.

Chapter 5

Formulation of models

There exists two classes of explanation for the origin of the visible PL and EL in P-Si, the quantum confinement effects and the surface state effects. Here we consider the hybrid model mixing the them to investigate EL.

5.1 The quantum confinement model (QCM)

This model is based on the electronic confinement in dot like structure of Si. The development of this model is based on the effective mass approximation theory. In this model, the luminescence process is attributed to an energy shift of carriers (electrons and holes) and is proportional to L^{-2} L being the Si-nc diameter [19, 30]. We model a nanoclustered QD by a sphere of diameter L , so that its HOMO-LUMO gap is [4, 35, 36, 37].

$$E_g^n = E_g^b + \frac{c_1}{L_1^{\alpha_1}} \quad (5.1.1)$$

Quantum wire can be modeled as a cylinder with HOMO-LUMO gap

$$E_g^n = E_g^b + \frac{c_2}{L_2^{\alpha_2}} \quad (5.1.2)$$

The energy in a QW is parabola, thus we can model it as a hemisphere so that its HOMO-LUMO gap is

$$E_g^n = E_g^b + \frac{c_3}{L_3^{\alpha_3}} \quad (5.1.3)$$

where E_g^n , E_g^b are the energy gaps of the confined and bulk structures respectively in their geometric domain; L_1 , L_2 , and L_3 are the diameters the sphere, the cylinder, and the

hemisphere which we model the QD, quantum wire and QW and c_1 , c_2 , c_3 , and α_1 , α_2 , α_3 are constants that can be found by empirical fit.

A natural choice to find QDs size is to associate the effective size with the diameter of the sphere which has the mass density ρ of bulk Si and contains the same number of Si atoms as the QD in question. Then the diameter is

$$L(N_{Si}) = \left(\frac{3}{4\pi\rho}\right)^{\frac{1}{3}} N_{Si}^{\frac{1}{3}} \approx 3.3685 N_{Si}^{\frac{1}{3}} A^0 \quad (5.1.4)$$

Assuming that a Gaussian size distribution about the mean diameter L_0 for the nanocrystallites;

$$I(L) = \frac{1}{\sqrt{2\pi\sigma}} \exp\left(-\frac{(L - L_0)^2}{2\sigma^2}\right) \quad (5.1.5)$$

The number of electrons in a column diameter L participating in the PL process is proportional to L^2 . The heights of the columns depend only on the growth time and are approximately the same. Hence

$$N_e \sim L^2 \Rightarrow N_e = bL^2$$

For a P-Si sample consisting of a varying column diameters the probability distribution of electrons participating in the PL process is;

$$I_{eL} = \frac{1}{\sqrt{2\pi\sigma}} N_e(L) \exp\left(-\frac{(L - L_0)^2}{2\sigma^2}\right) \quad (5.1.6)$$

$$I_{eL} = \frac{1}{\sqrt{2\pi\sigma}} bL^2 \exp\left(-\frac{(L - L_0)^2}{2\sigma^2}\right) \quad (5.1.7)$$

where b is a suitable normalization constant. The luminescence intensity can be determined by the Fourier transform of eq.(5.1.7) to the energy axis as:

$$I(\Delta E) = \int I(L) \delta\left(\Delta E - \frac{c_1}{L^2}\right) dL \quad (5.1.8)$$

$$I(\Delta E) = \frac{b}{\sqrt{2\pi\sigma}} \int_0^\infty \delta\left(\Delta E - \frac{c_1}{L^2}\right) L^2 \exp\left(-\frac{(L - L_0)^2}{2\sigma^2}\right) dL \quad (5.1.9)$$

The Dirac delta function facilitates a straight forward integration.

Putting $y = \frac{c_1}{L^2}$ and apply the properties of Dirac delta function, the above integral will be transformed in to the form:

$$I(\Delta E) = \frac{1}{2} \frac{bc_1^{\frac{3}{2}}}{\sqrt{2\pi\sigma}} \int_0^\infty \delta(\Delta E - y)y^{\frac{-5}{2}} \exp\left(-\frac{L_0^2}{2\sigma^2}\left(L_0\sqrt{\frac{c_1}{y}} - 1\right)^2\right)$$

The above integral gives the intensity as a function of ΔE

$$I(\Delta E) = \frac{bc_1^3}{\sqrt{8\pi\sigma}} \Delta E^{\frac{-5}{2}} \exp\left\{\frac{-L_0^2}{2\sigma^2}\left[\left(\frac{\Delta E_0}{\Delta E}\right)^{\frac{1}{2}} - 1\right]^2\right\} \quad (5.1.10)$$

where ΔE is the energy shift due to the confinement given by;

$$\Delta E = h\nu - (E_g - E_b) \quad (5.1.11)$$

E_g being the bulk band gap of Si or Ge in this sample and E_b is the exciton binding energy, and $\Delta E_0 = \frac{c_1}{L_0^2}$, L_0 being the nanocrystal mean diameter and σ standard deviations. The values of E_g ranges from 1.11 eV to 1.17 eV for Si, depending on temperature; however, we took 1.12 eV for Si and 0.7 eV for Ge which is actually reported in most standard experiments at room temperature, while the value of E_b varies with nanocrystal radius of the sample ranging exponentially from 0.05 eV ($r=5$ nm) to 0.24 eV ($r=1$ nm).

The EL spectrum is caused by injection of strong electric field ε or current, the energy associated to this field is:

$$E = NZe\varepsilon L$$

where N is the number of nanocrystallite Si or Ge taken in the sample, Z is the number of electrons in each atom, ε is the external applied electric field responsible for EL, and L is the diameter of the single atom; since EL and PL occurs at the same energy, using the analogy of the PL spectrum model we can write the energy shift as:

$$\Delta E = NZe\varepsilon L - (E_g - E_b) = NZVe - (E_g - E_b) \quad (5.1.12)$$

where V is the voltage applied to the nanocrystal sample and e is the charge of electron.

According to the QC model, the emission wavelength and intensity depends on nanocrystal diameter, size distribution and concentration. This model can explain the general tendency of most experimental results such as the blue shift of the luminescence spectrum with decrease of the Si-nc size. The QC model is highly predictive when the nanoclusters are isolated from the matrix (e.g; Si-nc isolated from SiO_2). Consequently this model does not give a satisfactory explanation for the evolution of the luminescence spectra for some experimental parameters such as the PL for sample temperature below 100K, as well as oxidation or oxygen passivation of samples containing Si-nc. Due to this reason we used another model for terminated Si-nc [25].

5.2 Surface state model (SSM)

Efficient emission from anodically etched surface layers on Si is a remarkable experimental effect. The fact that this light is emitted at room temperature raises the prospects for making Si based device structures. The large energy relaxation between the original excitation and the luminescence is described in terms of a diffusive drift of the exciton to a position of the lowest energy in the connected network of cylinders.

Very long relaxation times decreasing luminescence intensity at low temperature (1-30 K) is assigned as a singlet-triplet excitonic effects in the QC model. In terms of surface state model, the elementary excitations, electrons and holes are frozen out in spatially separated traps of a given crystallite grain.

The essential difference of the two models lies in the fact that in the pure quantum picture, the nanometer-sized Si particles have perfect surfaces. The surface Si bonding is unperturbed and electronic states are like those of quantum wells in conventional semiconductor hetrostructures.

In considering luminescence of a particle excited at high energy, there will be a radiative process from the extended bulk like states. This occur prior to trapping in a

surface-perturbed level. It is well known that EL spectrum, in particular the relative strength of the current-voltage (I-V) doublet and exact shape and position of the V-peak, depends on the doping, temperature, the excitation conditions, and the kind of hot electron-damage of Si-SiO₂ interface incurred prior to taking the emission spectrum. The relation of I-V characteristics of P-Si to those of bulk Si is so important that we show the example of EL from a forward biased p-n junction.

Very long times can be expected for the surface state mechanism when both electron and hole relax to confined and spatially separated states at low temperature. Recombination is then by tunneling only. Just like for Si-H, the radiative efficiency must decrease in this case. The surface state model can explain very long times at low temperatures without making use of exciton spin state. The spectrum of energy states also distinguishes the QC model from the surface state mechanism. A QD has unique lowest energy of the conduction band and highest valence state. The effective gap E_g^* is well defined. Only because there is a distribution of sizes and shapes for the dots, the optical absorption does not have sharp onset. The surface state model, tail of energy similar to what occurs in a Si-H. The resulting spectrum should extend over along energy range and should decay exponentially below E_g^* . One finds for P-Si that efficiently luminescing at 1.7 eV the broad and exponentially decaying absorption tail extending from 2.3 eV down to 1.4 eV.

The absorption spectrum and the fact that the luminescence occurs far down on the exponential tail require an explanation. According to the QCM the tail is linked with the distribution of particle size. In terms of SSM, the absorption is a measure of exponentially decreasing tail states with small additional effects of the size distribution [4].

5.2.1 Interface states model (ISM)

Amorphous SiO₂ has a direct band gap larger than 8 eV, which can not contribute to the visible luminescence spectrum. However, it can attribute to create a nobel electronic state in the Si-nc/SiO₂ interface due to the interconnection of the Si-nc with the SiO₂ by

the oxygen atoms. In this case the exciton can be confined in the interfacial layer between two regions of higher energy of amorphous and SiO_2 and Si-nc. In this model, named the three region model, the e-h pair produced in the Si-nc by photonic excitations, recombine at the interface after the emission of one or more phonons.

It is based on these facts that the Si-nc are generally in contact with other elements such as SiO_2 . Consequently, the interface always plays an important role in the system. However, it could be possible to attenuate the interface effect, for example by H-terminating the Si bonds at the Si-nc edge when Si-nc are H-terminated, there is evidence that light absorption and light emission occurs essentially in the Si-nc core states. We combined the ideas of QCM model and SSM to get our result.

In this chapter we formulated the two specified models to study EL and PL intensities from Si and Ge nanostructures, using the two models let us study the results of EL and PL emitted from Si and Ge nanostructures.

Chapter 6

Results and discussion

In this chapter we will study the results of EL intensities for Si and Ge nanostructures as a function of different parameters; We begin from the result of PL intensity, because we develop our models from the back ground knowledge of PL. We used the ideas and expression of our models and develop matlab programs to compute the EL intensity as a function of different parameters and we fit most of our results with experimental results reported in many experimental researches. All physical quantities in this result expressed in SI units unless specified.

6.1 Dependence of PL intensity on wavelength for different σ s

Fig 6.1 shows the PL intensity as a function of wavelength for both Si and Ge nanostructures.

As we can see from the figure, the PL intensity for both nanostructures seems to be almost similar since they have the same band structure except a slight change in the band gap energy. The standard deviation from the mean crystallite (which in fact contains the dependence of PL intensity on size) influences on the intensity.

Putting different values of sigma suppresses the nature of the luminescence intensity that would have been on the smaller value of sigma in the spectrum of luminescence intensity versus wavelength. This is as expected because the PL intensity depends on

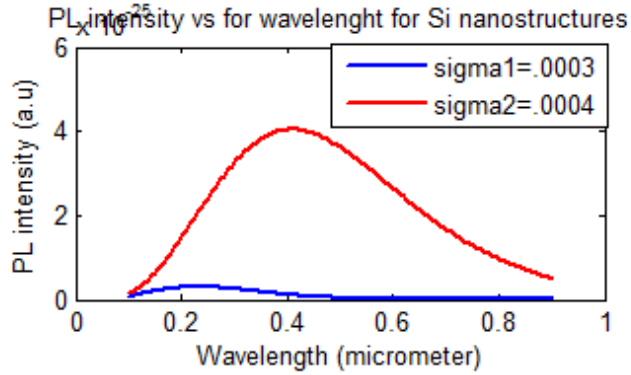


Fig. 6.1(a)

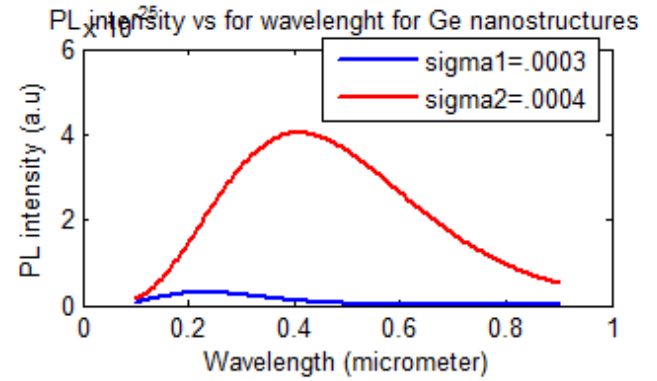


Fig. 6.1(b)

Figure 6.1: PL intensity versus wavelength for Si and Ge nanostructures

the emitted photon energy, not to the number of emitted photons. To argue our result is correct we can compare with the experimental result fig.6.3.

6.2 Dependence of EL intensity on wavelength for different σ s

Fig 6.2 shows the EL intensity as a function of wavelength for both Si and Ge nanostructures. The fig show most properties observed in PL intensity.

When we compare our result of fig.6.2 and the experimental result fig.6.3 nearly the same, yet still it seems to have difference on the nature of the curve; the difference arises here because we took different values of σ on the axis. If we do for single σ , the nature

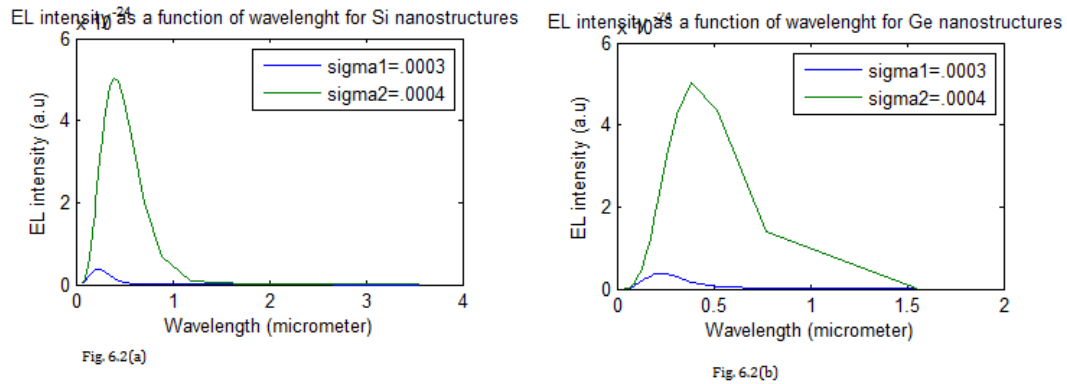


Figure 6.2: EL intensity as a function of wavelength for Si and Ge nanostructures

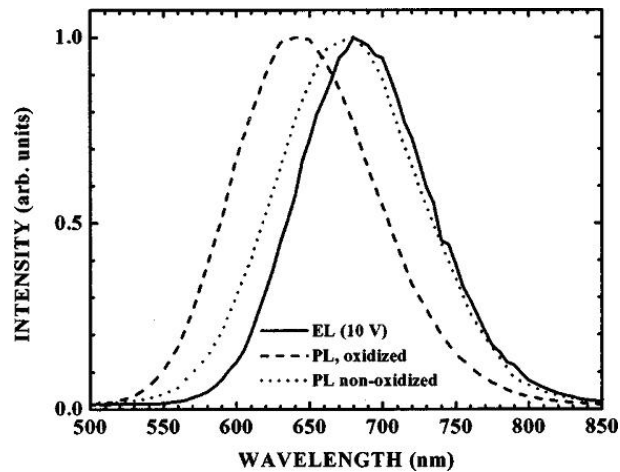


Figure 6.3: EL intensity versus wavelength taken for comparison [38]

of the curve looks like exactly the same as the result of experimental curve. When we compare fig.6.1 and 6.2 it seems that the EL spectrum and the PL spectrum have the same luminescence center, but the EL intensity has more sharp peak than the PL intensity this is also what experimental result reports.

6.3 EL intensity and number of sample atoms for Si and Ge nanostructures

Changing the number of atoms means changing the size of the nanocluster, which in turn changes the EL intensity.

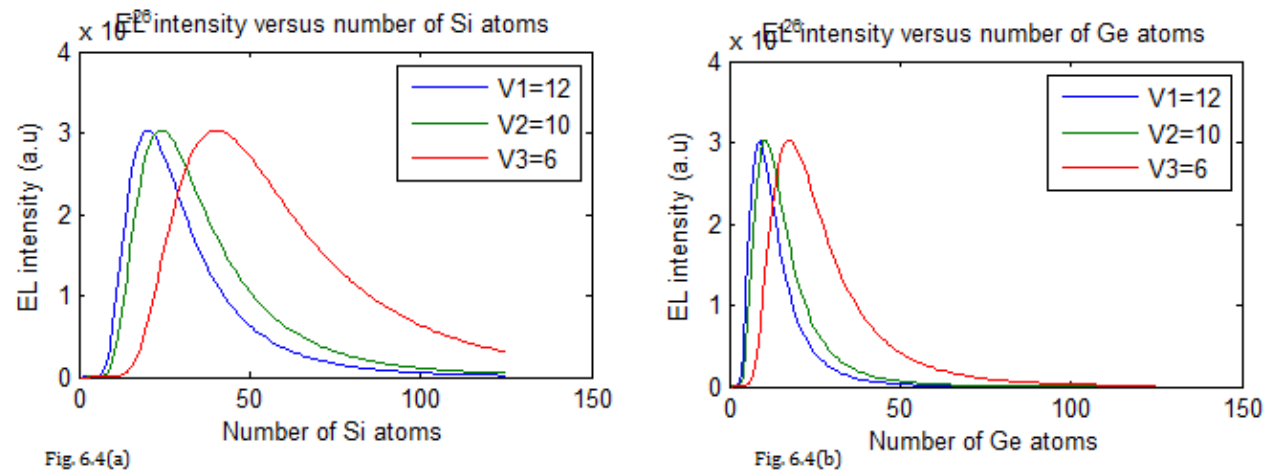


Figure 6.4: EL intensity versus number of Si and Ge nanoclusters

We have to select the number of samples we take based on the applied voltage and wavelength. For a fixed value of voltage our sample selection should be in such a way that to get EL spectrum in the visible range. If we choose too large or too small sample for a fixed voltage, the EL spectrum will lie in the ultraviolet or infrared region respectively, which has no physical utility for applications.

6.4 EL intensity and voltage

The EL intensity increases as the voltage applied to the nanocluster increases, yet to have a spectrum in the visible range we need to select the appropriate range of values

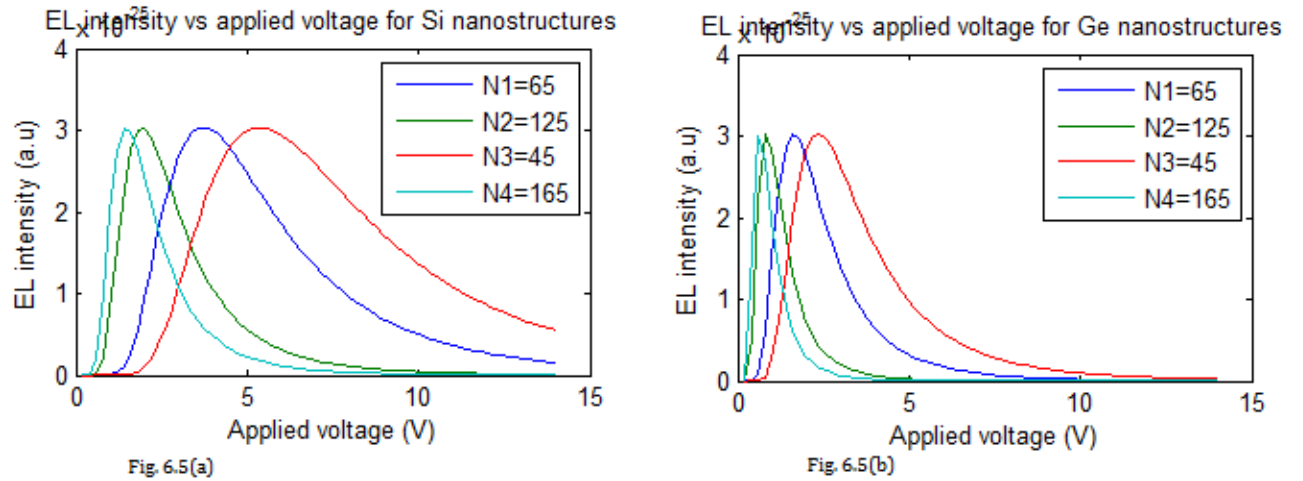


Figure 6.5: EL intensity versus applied voltage for Si and Ge nanoclusters

of voltage. Low voltage (< 6 V) is needed for good quantum efficiency and visible EL spectrum.

6.5 EL intensity and wavelength for oxygen terminated Si nanocluster

The EL intensity depends on the wavelength, voltage and the amount of O-bonded to Si. Here we assume SiO_2 , Si/ SiO_2 interface as a nanocluster. The band gap of SiO_2 , is about 8 eV for 3.7 nm thick crystallite, this large energy gap makes the spectrum out of the visible range as a result SiO_2 acts as an insulating material in which Si can be embedded in it to reduce the band gap so that for the size the band gap energy of Si/ SiO_2 is 1.7 eV which emits light nearly in the visible range. Thus SiO_2 layer does not contribute to the

visible PL or EL, however it is pointed out that this layer creates an electronic state in an interface region between crystalline Si core and SiO₂ layer. The band gap energy of 3.7 nm diameter Si crystallite is about 2.4 eV, which is roughly equal to the peak energy of the blue-green luminescence spectrum. The band gap of oxygen induced surface state

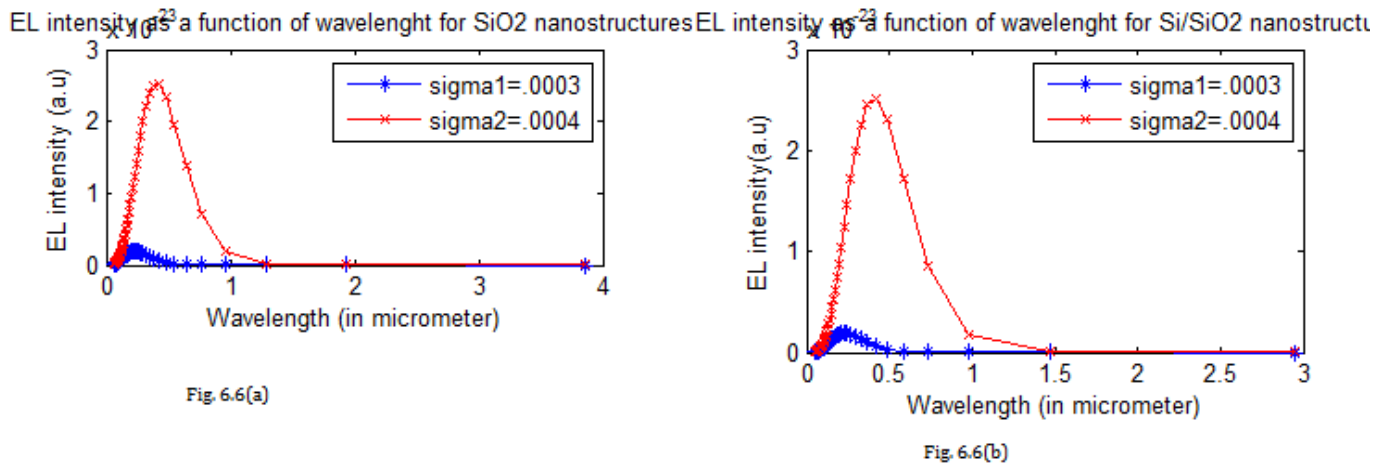


Figure 6.6: EL intensity as a function of wavelength for O-passivated Si nanoclusters

is lower than that of the crystalline Si core. Our result of surface Si-monolayer decreases with increasing the oxygen covering. The graphs of fig. 6.6 (a and b), which are based on these numerical values and plotted according to the QCM and SSM, agrees with the experimental result of fig. 6.2 .

6.6 EL intensity and wavelength for H-terminated Si nanocluster

Fig. 6.7 shows the dependence of EL intensity on wavelength for H-terminated Si nanocluster; termination with hydrogen changes the surface effects of Si nanocluster and deforms the structure; the band gap of H-terminated Si nanocluster is 2.6 eV, due to the shift in band the the dependence of EL intensity for H-terminated Si-nc is blue shifted

compared to the pure Si-nc. For Si-H cluster, the radiative recombination decreases since

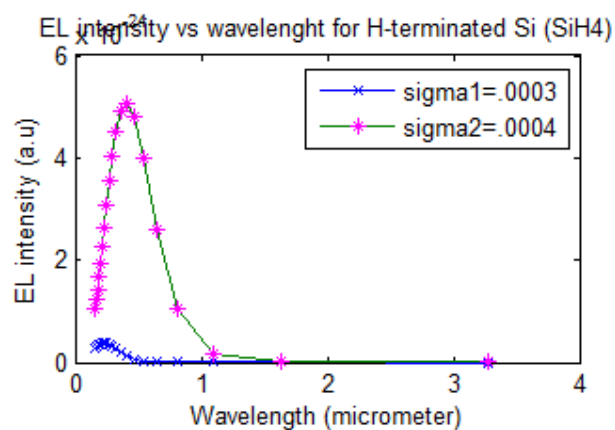


Figure 6.7: EL intensity as a function of wavelength for H-passivated Si nanoclusters

recombination is possible by tunneling only.

6.7 Dependence of EL intensity on Si-O bonds

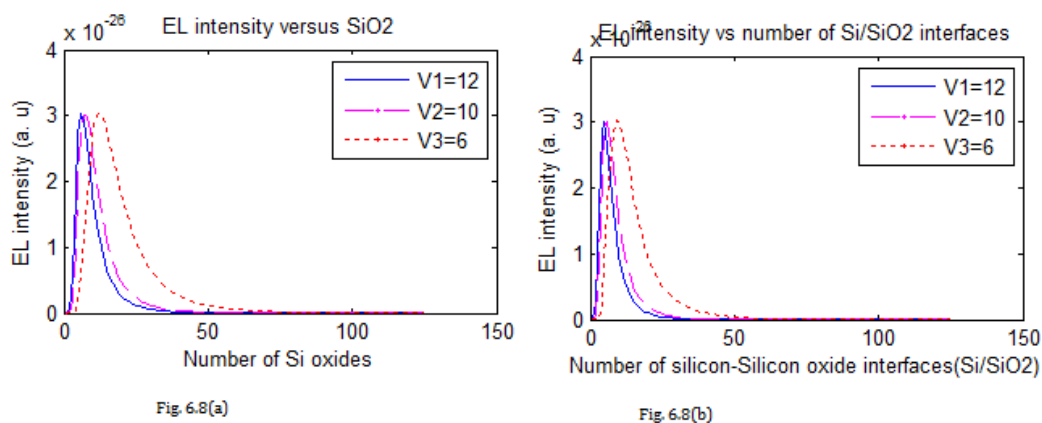


Fig. 6.8(a)

Fig. 6.8(b)

Figure 6.8: EL intensity versus number sample Si-O bonds

Fig. 6.8 (a and b) shows the effect of dangling bonds at the surface on the EL intensity.

The amount of Oxygen terminated and the number of SiO₂ sample changes the size of the cluster, which in turn changes the EL intensity.

6.8 Dependence of EL intensity on applied voltage for O-terminated Si

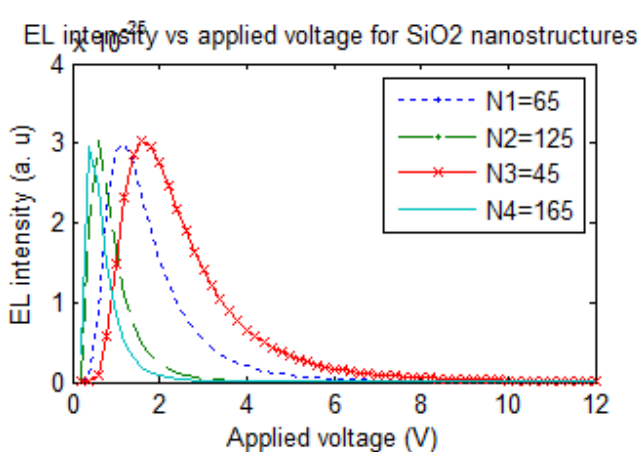


Fig. 6.9(a)

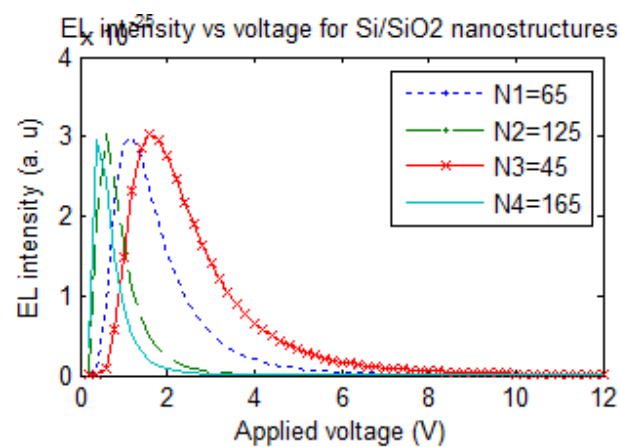


Fig. 6.9(b)

Figure 6.9: EL intensity as a function of applied voltage for O-passivated Si nanocluster

The dependence of EL intensity on voltage for O-terminated Si is slightly blue shifted compared to its dependence on voltage for pure Si nanocluster, this slight difference is due to the surface effects of the dangling bonds.

6.9 EL intensity versus Si-H bonds and voltage

Fig. 6.10(a) and fig. 6.10(b) shows the explicit relation between EL intensity versus number of Si-H bond and EL intensity versus voltage respectively for SiH_4 sample. The

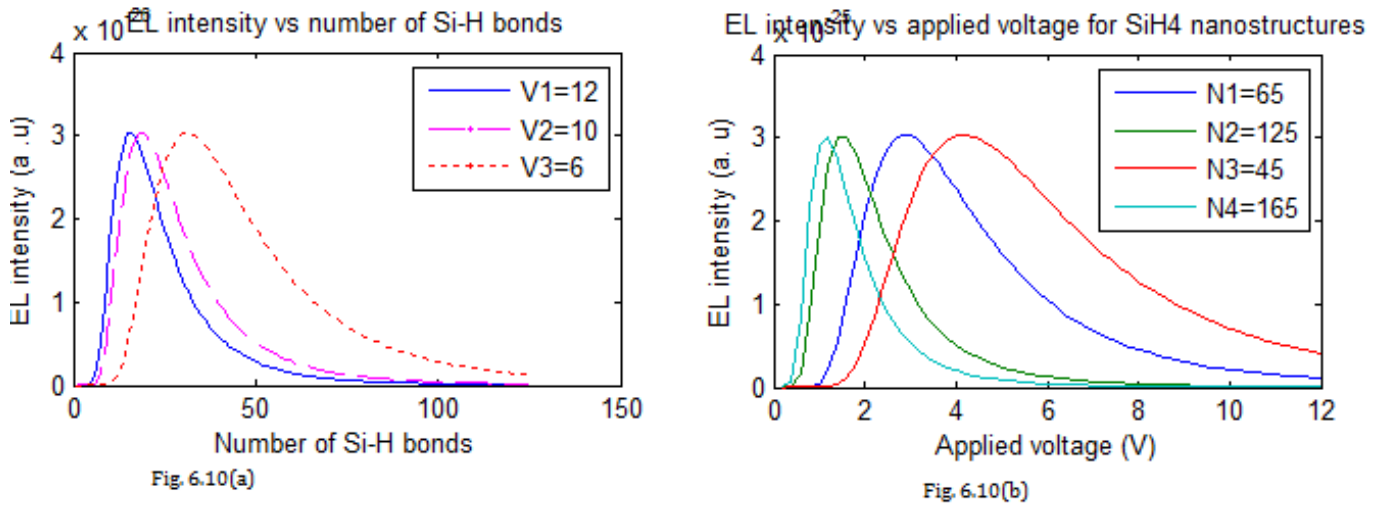


Figure 6.10: EL intensity vs wavelength for H-passivation

presence of e-h pair in the cluster causes a strong deformation of the structures with respect to their ground state configuration, and this is more evident for smaller systems. This is what we expect, since for large clusters charge density perturbation is distributed through out the structure.

6.10 Dependence of EL intensity on temperature and current density

The EL intensity depends on temperature for both pure Si nanoclusters, O-terminated, and H-terminated. For pure Si cluster the dependence is given by eq. (4.6.1) with specified values of E_1 and E_2 , where as for impure Si, it is related to the current density which in turn has a direct relation to the intensity. Here specially for SiO_2 being it is a

dielectric matrix we need to incorporate the dielectric constant and the barrier potential at the interface in the current density which is given by eq. (4.6.2). If we observe the

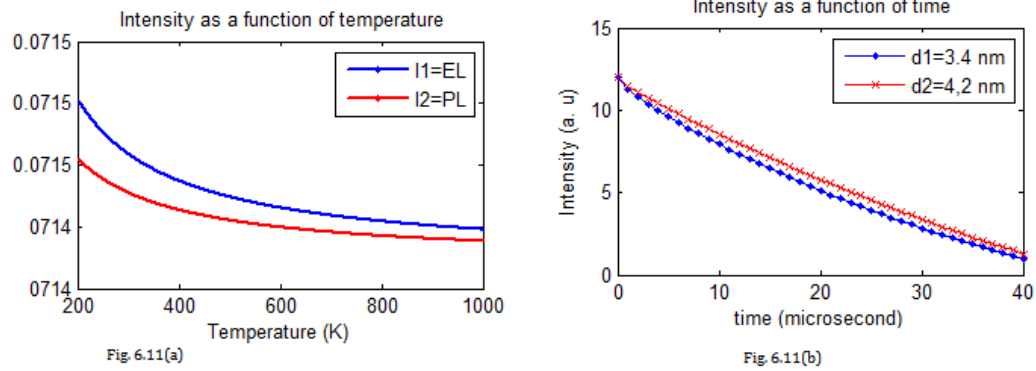


Figure 6.11: EL and PL intensities vs temperature

experimental result of fig. 4.5 and our result fig. 6.11(a), they are almost the same. In our result the size of the cluster is absorbed in the energy. Fig.6.11(b) shows the time dependence of EL intensity for 3.4 nm and 4.2 nm QDs at a time constant of $20\mu\text{s}$; the intensity is given by a stretch exponential decay.

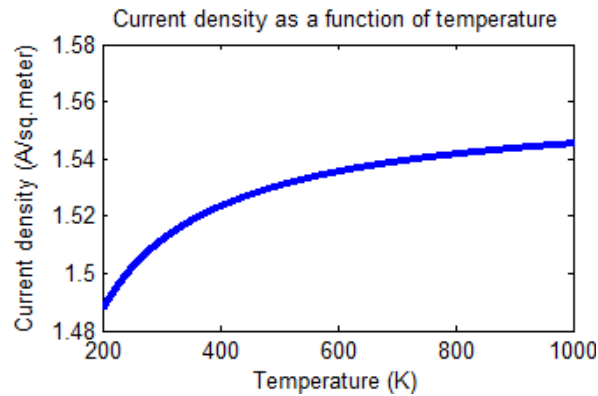


Figure 6.12: Current density vs temperature

In general we can summarize our result on the following bases:

Efficiency and voltage dependence of current density and EL intensity

The increase of η is mainly enhancement of carrier injection efficiency in to luminescent crystallites. As the voltage increases from 6 V to 12 V (fig.6.10), despite a slight increase in EQE, the power efficiency decreases. This shows that the power efficiency is very sensible to the applied voltage and that low voltage is necessary to obtain high efficiency. Oxidation improves the EL intensity, the effect of oxidation is to decrease the current density.

Spectral characteristics

- EL is red shifted compared to PL
- PL is blue shifted compared to EL
- Termination of Si with H and O (fig.6.6 and 6.7) induces a blue shift in the EL and PL spectrum
- The EL spectrum shape is similar to the PL one showing that the two phenomena has the same origin, namely recombination of carriers confined in to the crystallite.
- The range of the spectrum depends on the HOMO-LUMO gap.

Stability

Both EL intensity and current density increases, reaches maximum, and decreases very slowly as a function of time. In fact, since the EL intensity tends to reach a constant value, EL can be observed at room temperature for several hours.

Oxidation treatment improves the stability of the EL intensity. The stability of oxidized device is higher than non-oxidized device. Hydrogen desorption introduces non-radiative centers where responsible for the degradation of QE. The voltage needed to obtain a given current density and EL intensity increases with storage time.

Chapter 7

Conclusion and future outlook

QC effect is more prominent in Si and Ge nanostructures, its effect is the enhancement of radiative recombination rate of excitons with decreasing the cluster size, it also increases the band gap. PL and EL spectrum are caused by optical and electrical excitations respectively, has the same luminescence center, and occurs at the same energy; however, the EL spectra has more narrow Gaussian sub peaks and red shifted than the PL spectra. A blue shift to the luminescence is observed with decreasing nanocrystal size. Visible light emission in Si becomes possible with radiative recombination rates. The light generated by e-h recombination in Si and Ge nanostructures is quantified by quantum efficiency.

Generally the HOMO-LUMO gap determines the energy of emitted photon spectrum, the intensity of this spectrum depends on the size of the nanocluster and the energy shift due to confinement. The EL intensity depends on applied voltage, current density, temperature, time, size, and nature of the nanocluster sample taken. It is observed that the power efficiency is very sensible to the applied voltage, and low voltage is ($< 6V$) is necessary to obtain high efficiency and visible EL spectrum. EL always shows either reversible or permanent degradation with time, stability of EL intensity can be improved by termination of Si with O or H.

EL spectrum is independent of the applied injection current; however the EL intensity increases linearly with the applied injection current density.

Our result is inconformity with the experimental results, what makes it new is that

we formulate models and develop programs for our model (our result is computational) and we tried to hybrid the QCM and the SSM to explain the EL intensity from pure and Si terminated QD.

Future outlook

Study on the light emission properties (PL and EL) are the interesting application of Si and Ge nanostructures; detailed explanation on EL has not been done sofar. Electrophotoluminescence (EPL) and photoelectroluminescence (PEL) are also used nowadays, the future work will aim at studying the detail properties and applications of EL, PEL and EPL and enhancing the stability of EL intensity, increasing the QE both in PL and EL, and minimizing the EL degradation. Controlling Auger recombination, which is bad for luminescence, and enhancing radiative recombination will be the future work. EL and PL spectrum from Si and Ge nanostructures occurs at the same energy, but EL is red shifted and has narrow Gaussian sub peaks, it is thought that non-radiative recombination (Auger decay) which is bad for quantum efficiency is responsible for this effect; However, adequate explanation for it still do not exist, so this will be one of the future work for researches on EL and PL spectrum from Si/Ge nanostructures.

The models we used sofar can not explain the ion influence-dependant shift of the PL and EL of the Si-nc, we need to propose another model called reactive nanocluster model. In this model, e-h pair is created in the Si-nc and generates phonons in order to reach the interface energy state, which is affected by the interaction of neighboring Si-nc via a thin SiO₂ layer separating two crystals. Thus an increase of ion influence reduces the distance between adjacent Si-nc and, consequently, the thickness of the SiO₂ layer that modifies the interface energy state; hence one of the future work will be on the formulation of this model to study PL and EL.

Bibliography

- [1] www.ringsurf.com/online/2003-structures.html
- [2] [http://www.itrs.net/common/2005 ITRS/interconnect 2005.pdf](http://www.itrs.net/common/2005%20ITRS/interconnect%202005.pdf)
- [3] Hirschman, K. D. Tsybeskov, L. Dutttagupta, S. P and Fauchet P.M 'Silicon based visible light emitting devices integrated in to microelectronic circuits',nature **384**, 338 (1996)
- [4] L. T. Canham, *Silicon quantum wire fabrication by electrochemical dissolution of wafers*, Appl. phys. lett. **57** , 1046.
- [5] Wikipedia, the free encyclopedia.mht
- [6] Daniel Miloni, *Nanotechnology applications to telecommunications and networking*, John Wiley and Sons, Inc. 106 (2006).
- [7] Charles Kittel *Introduction to solid state physics*, John Wiley and Sons, Inc., New York, eighth edition 174 (2005).
- [8] Daryoush Shiri, Yifan Kong, Anderi Buin, and M. P. Anantram, *Strain induced change of bandgap and effective mass in silicon nanowires*, Appl. Phys. Lett. **93**, 073114 (2008)
- [9] L. Pavesi, P. Bettoti, M.Cazzanelli, Gam90 *Silicon nanostructure for photonics*
- [10] Jasprit Singh, *Electronic and optoelectronic properties of semiconductors* , New York, 54 (2003)
- [11] Edward L. Wolf, *Introduction to modern concepts in nanoscience*, Wiley-VCH, 40 (2004)

- [12] Neil W. Ashcroft, N. David Mermin, *Solid state physics*, Holt Rinehart and Wiston, New York, 175 (1976)
- [13] Donald A. Neamen, *Semiconductor physics and devices*, MCGraw-Hill, third edition, 72 (2003)
- [14] Yuri M. Galperin, *Introduction to modern solid state physics*, Blindern, Oslo, 47
- [15] Nenad Lilac, *Light emitting devices based on silicon nanostructures*, KTH, Royal intstitute of technology, Sweden.
- [16] icecube.wisc.edu/~morse/phy-spr06/lecture/244lec34.doc.
- [17] Zhenchan Feng, Raphael Tsu, *Hand book of porous silicon*.
- [18] <http://en.wikipedia.org/wiki/luminescence>.
- [19] G.G Ross, D. Barba and F. Martin *Structure and luminescence of silicon nanocrystals embedded in silicondioxide*, Int. J. Nanotechol. **5**, 9/10/11/12/, (2008)
- [20] JLin. GQyao, YQ Duan and GG Qin, *Ultraviolet light emission from oxidized porous silicon*, Solid state communications **97**, 3, 221 (1996)
- [21] Jwang, H-B jiang, W. C. Wang, J-B, Zheng, F-U Zhang, P-H Hao and X. Wang, *Efficient infrared-up-conversion luminescence porous silicon: Quantum confinement induced effect*, Physical Review letters **69**, 22, 3252 (1995).
- [22] J. Diener, M Ben-chorin, DI Kovalev, SD Ganichev and F. Koun, *Light from porous silicon by multiphoton vibronic excitation*, Physical Review B **52**, 8617 (1995).
- [23] Rebohle, J.Von Borany, H.Frob, W. Skorupa, Appl. Phys.B **71**, 131 (2000)
- [24] <http://en.wikipedia.org/wiki/electroluminescence>
- [25] D. R Vij, *Hand book of electroluminescent materials*, Institute of physics, Great Britian, (2004) (<http://www.physicsnetbase.com/ejournals/books/book-summary/summary.asp>)

- [26] N. Daldosso, M. Luppi, S. Ossicini, E. Degoli, R. Magri, G. Dalba, P. Fornasini, G. Grisenti, F. Rocca, L. Pavesi, S. Boninelli, F. Priolo, C. Spinella, and F. Iacona, *Role of interface region on the electronic properties of silicon nanocrystals embedded in silicon dioxide*, Phys. Rev B **68**, 085327 (2003).
- [27] Alessia Irrera, Fabio Iacona, Isodiana Crupi, Calogero D Presti, Giorgia Franzo, Corrado Bongiorno, Delfo Sanfilippo, Gianfranco Di Stefano, Angelo Piana, Pier Giorgio Fallica, Andrea Canino and Francesco Priolo, *Electroluminescence and transport properties in amorphous silicon nanostructures*, Nanotechnology **17**, 1492 (2006)
- [28] Eun-Chelcho, Martin A. Green, Gavin Conibeer, Dengyuan Song, Youth-Hyuncho, Giuseppe Scardera, Shujuan, Sang Wook park, X. J. Hao, Yidan Haung, and Lap Van Dao., *Silicon quantum dots in a dielectric matrix for all silicon Tandem solar cells*, Research Article 69578, 11 (2007)
- [29] Tai-Cheng Tsai, Li-Zhen Yu and Ching-Ting Lee, *Electroluminescence emission of crystalline silicon nanoclusters grown at low temperature*, Nanotechnology **18**, 275707 (2007)
- [30] Minoru Fujii, Osamu Mamezaki, Shinji Hayashi and Keiichi Yamamoto, *Current transport properties of silicon dioxide films containing Ge nanocrystals*, J. Appl. Phys. **83**, 3 (1998)
- [31] Elena Degoli, G. cantele, Eleonora Luppi, Rita Magri, D. Ninno, O. Bissi, and Stefano Ossicini, *Ab-initio structural and electronic properties of hydrogenated silicon nanoclusters in the ground and excited states*, Physical Review B **69**, 155411 (2004)
- [32] Bhushan, *Hand book of nanotechnology*, Springer
- [33] L. Tsybeskov, Review Article 218032, 16 (2008)
- [34] V. Agarwal et al., *PL spectra and temperature dependence in self supporting porous silicon*, Phys. Stat. sol. **182**, 385 (2000)
- [35] J. P. Proot, C. Delerue, G. Allan, Appl. Phys. Lett. **61**, 1948 (1992)

- [36] S. Prezioso, A. Anochenko, Z. Gaburro, L. Pavesi, G. Puncker, L. Vanzetti, and P. Bellutti, *Electrical conduction and electroluminescence in nanocrystalline silicon-based light emitting devices*, Journal of Applied Physics **104**, 063103 (2008)
- [37] A. Zunger, L. W. Wang, *Theory of silicon nanostructures*, Applied Surface Science, **102**, 350 (1996)
- [38] K. V. Shcheglov, C. M. Yang, K. J. Vahala, and Harry A. Atwater, Appl. Phys. Lett., **66**, 6 (1995) Applied Surface Science **102**, 350 (1996)
- [39] <http://science.hq.nasa.gov>
- [40] <http://www.nanoforum.org>
- [41] <http://www.nanohub.org>
- [42] <http://www.memsnet.org/material/silicondioxidesio2bulk>